protected from abrasion. Strands of wood fibers in coarse paper, or worse, the stick end of a cotton swab applicator, are strong enough to place dozens of permanent scratch marks (sleeks) on the front lens element with a single swipe. Once present, scratches cannot be removed, and their effect (even if hardly visible) is to scatter light and permanently reduce image contrast. Further, most lenses contain an antireflection coating composed of layers of a dielectric material; each layer is just a few atoms thick. Although antireflection surfaces are protected with a layer of silicon monoxide, you should use only high-quality lens tissue and apply only a minimum of force to wipe off drops of excess oil.

Mechanical Force

Never apply strong physical force to an objective lens or other optical component. To bring another objective into position, move the rotating turret; do not grab and pull on a lens to bring it into position. Also, never remove a stuck objective with a vice-grips or a pipe wrench! If the threads of an objective become stuck to the rotating turret from dried culture medium, oil, or corrosion, apply a drop of water or lens cleaner or penetrating oil to loosen the objective and avoid using force. Likewise, never drop an objective onto the lab bench or floor. Also, do not allow an objective to strike exposed edges of the microscope stage or the condenser (easy to do on some inverted microscope designs). Impacts of this kind cause two forms of irreparable damage: (1) They can crack the compounds that seal the top lens element and metal lens cap, thus allowing immersion oil to penetrate into the lens and coat internal lens elements, causing permanent damage. (2) They can induce permanent stresses in the glass lens components of an objective and may severely degrade its performance in sensitive forms of light microscopy that use polarized light.

Exercise: Constructing and Testing an Optical Bench Microscope

Microscope Construction and Testing

Determine the focal lengths of the lenses using the method described in the text and label them with pieces of lab tape applied to their edges. Use three 50 mm lenses for the objective, ocular, and illuminator s collector lens to construct the optical bench microscope.

Mount in order of sequence on the optical bench: a tungsten lamp illuminator, 50 mm collector lens, specimen holder, objective lens, and ocular.

Handwrite the letter *a* with a fine marker pen on a sheet of lens tissue or on a microscope slide, and tape it to the specimen holder, centering the letter on the optic axis.

Position the collector lens about 75 mm away from the lamp filament. Position the specimen about 20 cm away from the collector lens. The light from the illuminator should be focused into a 1 2 cm diameter spot centered on the object (the letter *a*).

Using the lens equation $1/f = 1/a + 1/b$, calculate the object-lens distance that gives an image-lens distance of ~30 cm, and mount the objective lens at the calculated position.

Place a sheet of paper (a paper screen) at the 30 cm location to confirm that the intermediate image of the letter *a* is both real and magnified. Notice that the real intermediate image is both inverted and upside-down. Confirm that it is necessary to position the lens between 1 and 2 focal lengths away from the object to obtain a real intermediate image of the object.

Mount the ocular at a position that gives a magnified image of the letter when looking down the axis of the microscope through the ocular. The eye might have to be positioned several inches behind the ocular to see the specimen clearly. Note the image ocular lens distance.

Place a paper screen in the plane of the virtual image to confirm that it is indeed virtual that is, no image is produced on the screen. You have now created a compound light microscope!

Answer the following questions about your microscope:

1. Is the object located precisely at the focal length of the objective lens?
2. Is the real intermediate image located precisely at the focal length of the ocular?
3. Explain why the eye-brain perceives a magnified virtual image, while the retina receives a real image from the ocular lens.

Lens Aberrations

Prepare a specimen consisting of a 5 cm^2 piece of aluminum foil with a dozen small pinholes contained within a 5 mm diameter circle, and mount it on the optical bench microscope. The ideal specimen has some pinholes on or close to the axis and other pinholes near the periphery of the field of view. What lens aberrations do you observe while examining the pinhole images? Here are some tips:

Chromatic aberration: Move the objective lens back and forth through focus and notice how the fringes around the points of light change color depending on the lens position.

Spherical aberration: Pinholes at the periphery of the visual field look blurry. The blurriness can be reduced by creating a 5 mm hole in an opaque mask and placing it in the back focal plane of the objective lens.

Coma and astigmatism: At best focus, peripheral pinholes look like streaks with comet tails that radiate from the center of the field (coma). As the objective is moved back and forth through the plane of best focus, the streaks become drawn out into elliptical shapes that change their orientation by 90° on each side of focus (astigmatism).

Distortion and curvature of field: At best focus, the focal plane is curved like the shape of a bowl, so only one zone of a certain radius can be focused at one time (curvature of field). To view pincushion or barrel distortion, replace the pinhole specimen with a fine mesh copper grid used for electron microscopy and examine the pattern of the square mesh of the grid on the viewing screen (distortion).

CHAPTER

5

DIFFRACTION AND INTERFERENCE IN IMAGE FORMATION

OVERVIEW

This chapter deals with diffraction and interference in the light microscope the key principles that determine how a microscope forms an image. Having just concluded a section on geometrical optics where image locations and foci are treated as points, lines, and planes, it is surprising to learn that in the microscope the image of a point produced by a lens is actually an extended spot surrounded by a series of rings and that a focal plane is contained in a three-dimensional slab of finite thickness. These properties are due to the diffraction of light (see Fig. 5-1). In the microscope, light from the illuminator is diffracted (literally broken up in the sense of being scattered or spread) by the specimen, collected by the objective lens, and focused in the image plane, where waves constructively and destructively interfere to form a contrast image. The scattering of light (diffraction) and its recombination (interference) are phenomena of physical optics or wave optics. We study these processes, because they demonstrate how light, carrying information from an object, is able to create an image in the focal plane of a lens. With a working knowledge of diffraction, we understand why adjusting the condenser aperture and using oil immersion techniques affect spatial resolution. Diffraction theory also teaches us that there is an upper limit beyond which a lens cannot resolve fine spatial features in an object. In studying diffraction, we see that complex optical phenomena can be understood in mathematically precise and simple terms, and we come to appreciate the microscope as a sophisticated optical instrument. Readers interested in the physical optics of diffraction and interference of light can refer to the excellent texts by Hecht (1998) and Pluta (1988).

DEFINING DIFFRACTION AND INTERFERENCE

Diffraction is the spreading of light that occurs when a beam of light interacts with an object. Depending on the circumstances and type of specimen, diffracted light is perceived in different ways. For example, when a beam of light is directed at the edge of an object, light appears to bend around the object into its geometric shadow, a region not directly illuminated by the beam (Fig. 5-2a). The situation reminds us of the behavior of

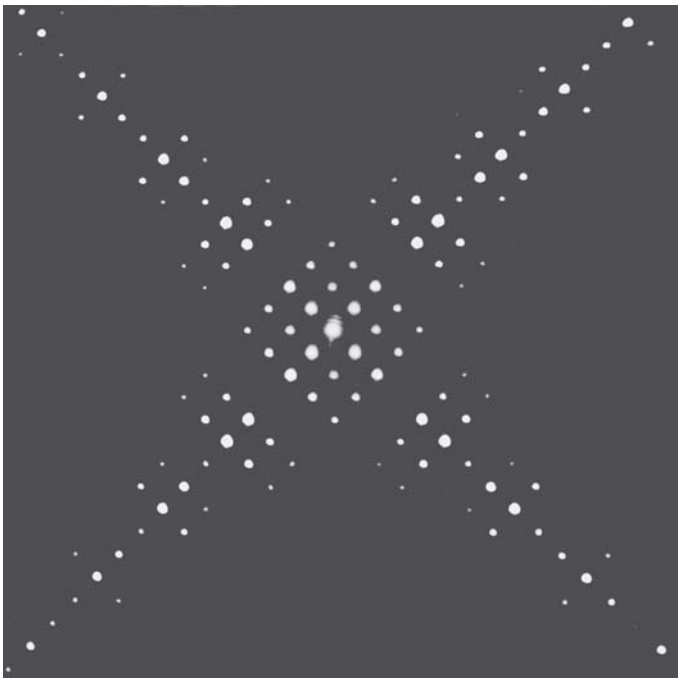

Figure 5-1
Diffraction image of a copper mesh grid. A 400-mesh grid was illuminated with a laser pointer, and its diffraction pattern was photographed on a projection screen. Multiple diffraction spots are observed due to the relatively large spacing between grid bars and the coherent laser light source.

water waves incident on a log floating in a pond. The waves wrap around the ends of the log into the geometrical shadow; instead of reflecting away from the ends of the log, they seem to grab hold of the ends and swing themselves around into the sheltered zone. The redirected component of diffracted light is easily observed when a tree or person is backlighted by a strong light source under conditions where the background behind the object is still dark; the bright line outlining the silhouette of the object is diffracted light. Of particular interest to us is the image of a point source of light in the microscope, since images are composed of a myriad of overlapping points. As we will see, waves emanating from a point in the object plane become diffracted at the margins of the objective lens (or at the edges of a circular aperture at the back focal plane of the lens), causing the image of the point to look like a spot. Thus, the image of a point in a microscope is not a point at all, but a diffraction pattern with a disk of finite diameter. Because of diffraction, an object s image never perfectly represents the real object and there is a lower limit below which an optical system cannot resolve structural details.

Diffraction is also observed when a beam of light illuminates a microscope slide covered with fine dust or scratches (Fig. 5-2b). The spreading of an automobile s headlight beams on a foggy night is another good example of the phenomenon. In these cases, diffraction is defined as the scattering of light by small particles having physical dimensions similar to the wavelength of light. The amount of scattering and angle of

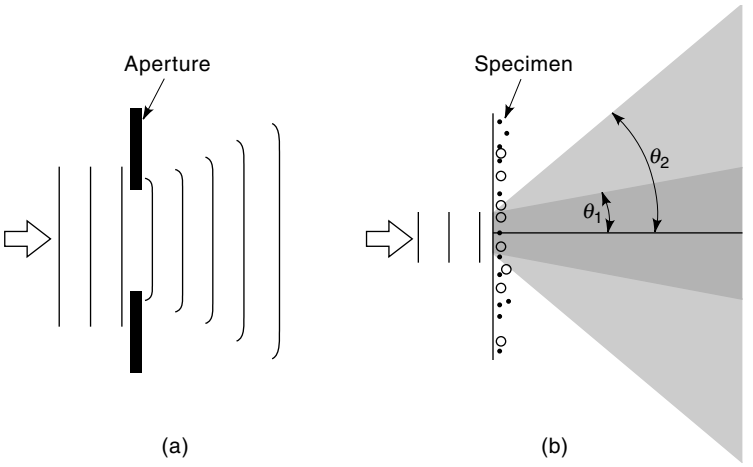

Figure 5-2

Diffraction at an aperture and at a substrate containing fine particles. (a) The electric field of a planar wavefront becomes disturbed by diffraction upon passage through an aperture. The waves appear to grab hold of the aperture and swing around into its geometric shadow. The amplitude profile of a transmitted wavefront is also no longer uniform and remains permanently altered after passage through the aperture (not shown). (b) A substrate containing a layer of a mixture of fine particles (0.2 and 2 μm diameter) diffracts an incident planar wavefront into scattered beams that diverge at different angles. The angle of spreading (θ) is inversely proportional to the size of the particles.

spreading of the beam depend on the size and density of the light-diffracting particles. In the case of illuminated specimens in the microscope, there are therefore two primary sites of diffraction: one at the specimen itself and another in the aperture of the objective lens. Image formation by a lens is critically dependent on these events. If light passes through an object but does not become absorbed or diffracted, it remains invisible. It is the spreading action or diffraction of light at the specimen that allows objects to become visible, and the theory of image formation is based on this principle.

Just as diffraction describes the scattering of light by an object into divergent waves, *interference* describes the recombination and summation of two or more superimposed waves, the process responsible for creating the real intermediate image of an object in the focal plane of a microscope. In a real sense, diffraction and interference are manifestations of the same process. The traditional way of describing interference is to show the recombination of waves graphically in a plot depicting their amplitude, wavelength, and relative phase displacement (Fig. 5-3). The addition of two initial waves produces a resultant wave whose amplitude may be increased (*constructive interference*) or diminished (*destructive interference*).

The term *interference* is frequently taken to mean that waves annihilate each other if they are out of phase with each other by λ/2, and indeed a graphical depiction of interfering waves reinforces this idea. However, since it can be demonstrated that all of the photon energy delivered to a diffracting object such as a diffraction grating can be completely recovered (e.g., in a resultant diffraction pattern), it is clear that photons do not self-annihilate; rather their energies become redistributed (channeled) during diffraction

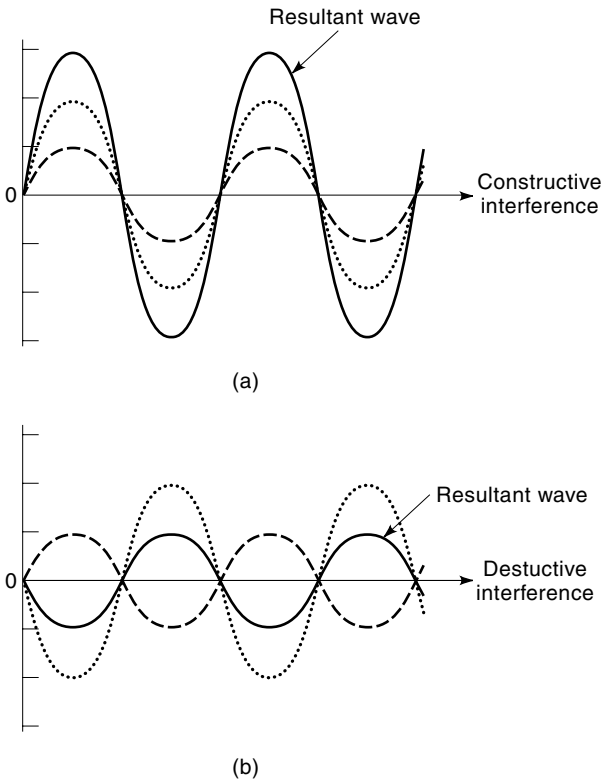

Figure 5-3

Two coincident waves can interfere if their E vectors vibrate in the same plane at their point of intersection. Two waves are shown that vibrate in the plane of the page. In these examples, both waves (dotted and dashed curves) have the same wavelength, but vary in amplitude. The amplitude of a resultant wave (solid curve) is the arithmetic sum of the amplitudes of the two original waves. (a) Constructive interference occurs for two waves having the same phase. (b) Destructive interference occurs for waves shifted in phase; if the amplitudes of the waves are the same and the relative phase shift is $\lambda/2$, the wave is eliminated.

and interference in directions that permit constructive interference. Likewise, interference filters do not destroy the light they do not pass; they merely reflect or absorb it. It is therefore best to think of diffraction and interference as phenomena involving the redistribution of light waves and photon energy. Accordingly, wave constructions of the kind shown in Figure 5-3 are best thought of as devices that help us calculate the energy traveling in a certain direction or reaching a certain point. The mechanism by which light energy becomes redistributed is still not understood.

THE DIFFRACTION IMAGE OF A POINT SOURCE OF LIGHT

The image of a self-luminous point object in a microscope or any other image-generating instrument is a diffraction pattern created by the action of interference in the image plane.

When highly magnified, the pattern is observed to consist of a central spot or diffraction disk surrounded by a series of diffraction rings. In the nomenclature of diffraction, the bright central spot is called the 0th-order diffraction spot, and the rings are called the 1st-, 2nd-, 3rd-, etc.-order diffraction rings (see Fig. 5-4). When the objective is focused properly, the intensity of light at the minima between the rings is 0. As we will see, no lens-based imaging system can eliminate the rings or reduce the spot to a point. The central diffraction spot, which contains ~84% of the light from the point source, is also called the *Airy disk,* after Sir George Airy (1801 92), who described some of its important properties.

The Airy disk pattern is due to diffraction, whose effect may be described as a disturbance to the electric field of the wavefront in the aperture of the lens the consequence of passing an extended electromagnetic wavefront through a small aperture. The disturbance continues to alter the amplitude profile of the wavefront as the front converges to a focus in the image plane. Diffraction (the disturbance) constantly perturbs the incident wavefront, and since no one has invented a lens design to remove it, we must accept its alteration of points comprising the image. The size of the central disk in the Airy pattern is related to the wavelength λ and the aperture angle of the lens. For a telescope or camera lens receiving an incident planar wavefront from an infinitely distant source such as a star, the aperture angle is given as the focal ratio *f/D,* where *D* is

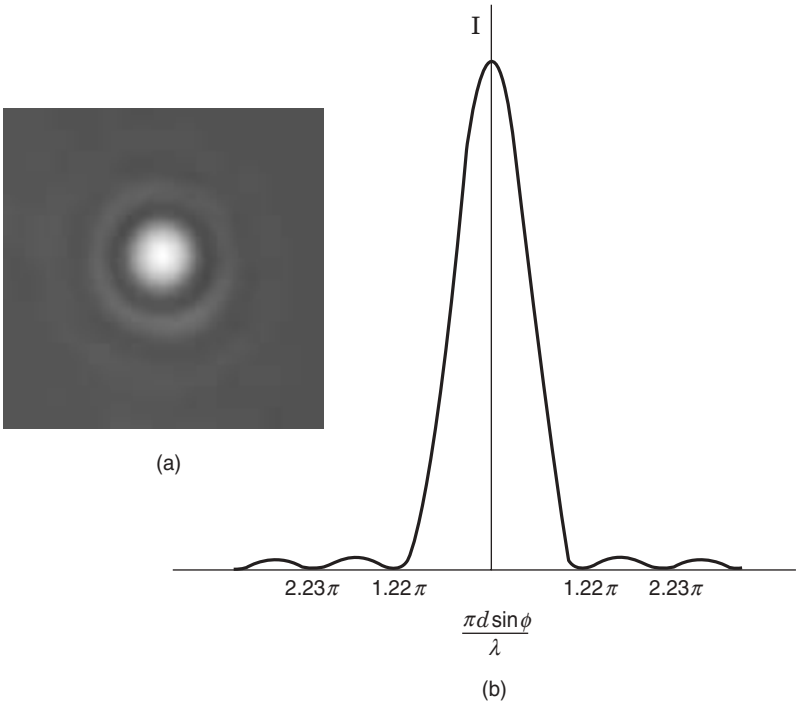

Figure 5-4

The diffraction pattern of a point source of light. (a) Diffraction pattern showing central diffraction disk surrounded by diffraction rings. (b) Intensity profile a diffraction spot. The central spot and surrounding rings are evident. The separation distance between the center of the spot and the first minimum depends on the angular aperture of the lens.

the lens diameter and f is the focal length. In this case, the *aperture angle* is the angular diameter of the lens as seen from a point in the image plane at focal length f. The size of the diffraction disk radius d is given by

$$d = 1.22\lambda\,(f/D).$$

In a microscope, the aperture angle is described by the numerical aperture NA, which includes the term $\sin\theta$, the half angle over which the objective can collect light coming from a nearby object. (NA is defined further in Chapter 6.) In the case of a microscope image, the radius d of the diffraction spot for a self-luminous point of light in the image plane is described by a related expression:

$$d = 1.22\,\lambda/2\mathrm{NA}$$

In both situations, the size of the spot decreases with decreasing wavelength and increasing numerical aperture, but always remains a disk of finite diameter. The spot size produced by a 25× oil immersion objective with NA = 1 is about 30 μm. Obtaining an image whose resolution is limited by the unit diffraction spot, rather than by scattered light or lens aberrations, is what is meant by the term *diffraction limited.* We examine the relationship between diffraction and resolution in Chapter 6.

Demonstration: Viewing the Airy Disk with a Pinhole Aperture

It is easy to observe the Airy disk by examining a point source of light through a pinhole (Fig. 5-5). This is best done in a darkened room using a bright lamp or microscope illuminator whose opening is covered with a piece of aluminum foil containing a pinhole that will serve as a point source of light when viewed at a distance of several feet. The illuminator s opening should be completely covered so that the amount of stray light is minimal. A second piece of foil is prepared with a minute pinhole, 0.5 mm diameter or less, and is held up to the eye to examine the point source of light at the lamp. The pinhole eye lens system (a pinhole camera) produces a diffraction pattern with a central Airy disk and surrounding diffraction rings. The same observation can be made outdoors at night examining distant point sources of light with just the pinhole held over the eye. This simple diffraction pattern is the basic unit of image formation. If the eye pinhole is made a little larger, the Airy disk becomes smaller, in accordance with the principle of angular aperture we have described. Now turn on the room lights and look through the pinhole at objects in the room, which look dim (not much light through the pinhole) and blurry (low resolution). The blurry image is caused by large overlapping diffraction spots of image components on the retina. When the pinhole is removed and the objects are viewed directly, the image is clearer because the larger aperture size afforded by the eye s iris and lens results in smaller diffraction spots and an increase in resolution and clarity. We begin to appreciate that an extended image can be viewed as the summation of a myriad of overlapping diffraction spots.

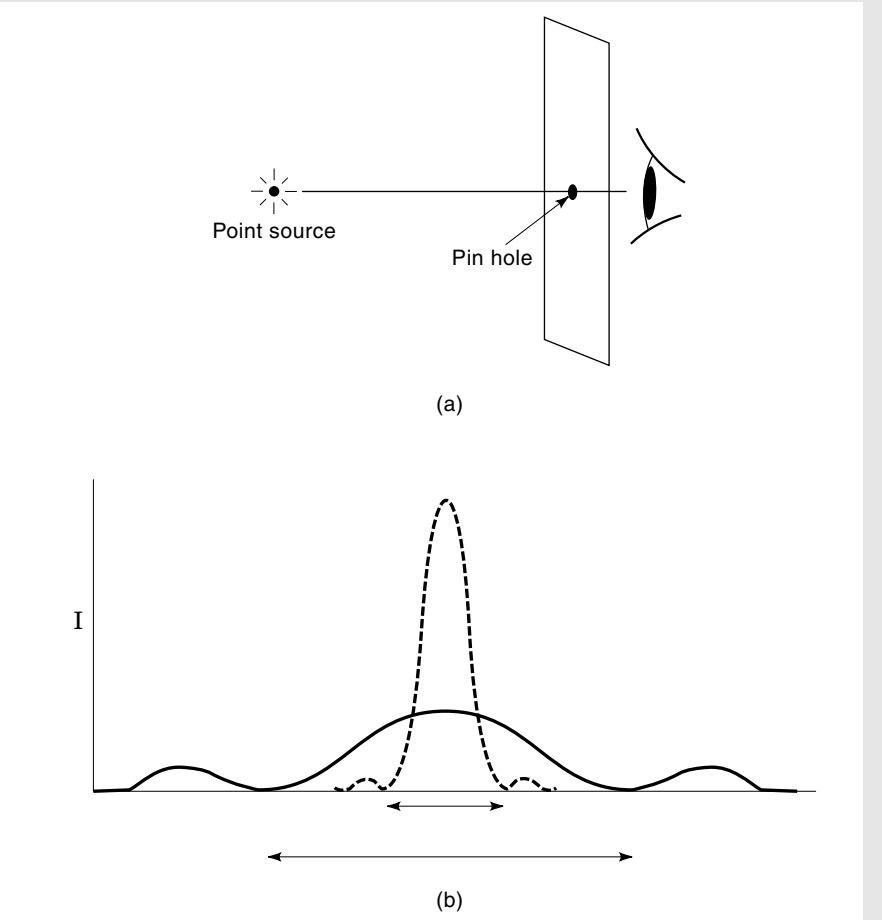

Figure 5-5

The image of a point source of light viewed through a pinhole is a perceptible disk. (a) Viewing a point source of light through a pinhole. (b) Relative sizes of the diffraction disk on the retina when a point source is viewed with normal vision (dotted line) and through a pinhole (solid line). With a pinhole, the diffraction disk expands about 10-fold to 30 40 μm, covering a patch of hundreds of cone cells on the retina, thereby allowing perception of a visible diffraction disk and surrounding rings.

In cameras and telescopes, the image of a star is likewise always a finite diffraction disk (not a point) with linear radius $r = 1.22\lambda$ (*f*/*D*), where *f*/*D* is called the *focal ratio* or *f*-number. Roughly, the diameter of the diffraction spot in μm is the focal ratio in millionths of a meter. Thus, the diameter of the diffraction spot in the primary focal plane of the 250 cm diameter, *f*/5 mirror of the Hubble space telescope is 5 μm. In the case of the human eye or photographic camera, the image of a point source on the retina or film has a diameter of about 3 μm. In all of these optical systems, the image of a point source corresponds to a diffraction disk, and the terms NA and *f*/*D* are measures of the effective

aperture angle and light-gathering ability. As shown in this chapter, the spatial resolution of the microscope is limited by the smallest disk that it is possible to obtain by varying λ and NA. Only when the images of specimen details subtend diameters greater than this limit can you begin to obtain information regarding the size, shape, and periodicity of the object.

CONSTANCY OF OPTICAL PATH LENGTH BETWEEN THE OBJECT AND THE IMAGE

Before we examine the effect of lens diameter on diffraction spot size and spatial resolution, we need to consider the concept of optical path length for an imaging system containing a perfectly corrected lens. In practice, microscope objectives and other corrected lenses only approximate the condition of being perfectly corrected, and waves arrive at the conjugate image point somewhat out of place and out of phase. This is usually not a serious problem. Despite practical limitations in finishing lenses with spherical surfaces, most microscope lenses give diffraction-limited performance with an average error in phase displacement (wavefront error) of less than $\lambda/4$, and manufacturers strive to obtain corrections of $\lambda/10$ or better. As is known, light from a self-luminous point in an otherwise dark specimen plane radiates outward as an expanding spherical wavefront; waves collected by the objective are refracted toward the center line of the lens and progress as a converging spherical wavefront to a single point in the image plane. However, it is also true and this point is critical for image formation that *the number of vibrations as well as the transit time experienced by waves traveling between an object point and the conjugate image point are the same regardless of whether a given wave passes through the middle or the periphery of the lens.*

Ideally, all waves from an object point should arrive at the image point perfectly in phase with one another. Given the large differences in the spatial or geometric path lengths between central and peripheral waves, this seems improbable. The explanation is based on the concept of *optical path length,* a length distinct from the geometric path length. It can be used to calculate the number of vibrations experienced by a wave traveling between two points. As it turns out, variations in the thickness of the lens compensate for the differences in geometric paths, causing all waves to experience the same number of vibrations (Fig. 5-6). It can also be shown that the transit time required for light to travel between object and image points along different trajectories having the same optical path length is the same. These concepts become important when we discuss the spatial and temporal coherence of light later in the chapter.

In optics, the *optical path length (OPL)* through an object or space is the product of the refractive index n and thickness t of the object or intervening medium:

$$OPL = nt.$$

If the propagation medium is homogeneous, the number of vibrations of a wave of wavelength λ contained in the optical path is determined as

$$\text{Number of vibrations} = nt/\lambda.$$

Since the frequency of vibration remains constant and the velocity of light $= c/n,$ when a wave traverses a lens of higher refractive index than the surrounding medium,

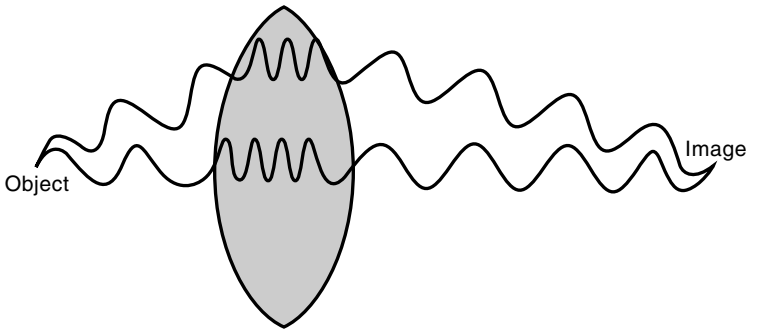

Figure 5-6
Preservation of the optical path length between the object and image. The optical path length may be regarded as the number of cycles of vibration experienced by a wave between two points. Two waves traveling in phase from a point in an object and entering the center and periphery of a lens cover different physical distances, but experience the same optical path length, and therefore arrive simultaneously and in phase at the conjugate point in the image plane. This occurs because the wave traveling the shorter geometric path through the middle of the lens is relatively more retarded in its overall velocity, owing to the longer distance of travel in a high-refractive-index medium (the glass lens). Note that the total number of cycles (the number of wavelengths) is the same for both waves.

the wavelength and velocity decrease during transit through the lens. Thus, the number of cycles of vibration per unit of geometrical distance in the lens is greater than the number of cycles generated over the equivalent distance in the surrounding medium. The overall optical path length expressed as the number of vibrations and including the portions in air and in glass is thus described as

$$\text{Number of vibrations} = n_1 t_1/\lambda_1 + n_2 t_2/\lambda_2,$$

where the subscripts 1 and 2 refer to parameters of the surrounding medium and the lens. As we will encounter later on, the *optical path length difference* Δ between two rays passing through a medium vs. through an object plus medium is given as

$$\Delta = (n_2 - n_1)t.$$

EFFECT OF APERTURE ANGLE ON DIFFRACTION SPOT SIZE

Now let us examine the effect of the aperture angle of a lens on the radius of a focused diffraction spot. We consider a self-luminous point P that creates a spherical wavefront that is collected by the objective and focused to a spot P' in the image plane (Fig. 5-7a). In agreement with the principle of the constancy of optical path length, waves passing through points A and B at the middle and edge of the lens interfere constructively at P'. (The same result is observed if Huygens wavelets [discussed in the next section] are constructed from points A and B in the spherical wavefront at the back aperture of the lens.) If we now consider the phase relationship between the two waves arriving at another point P'' displaced laterally from P' by a certain distance in the image plane, we see that a certain distance is reached where the waves from A and B are now 180° out of

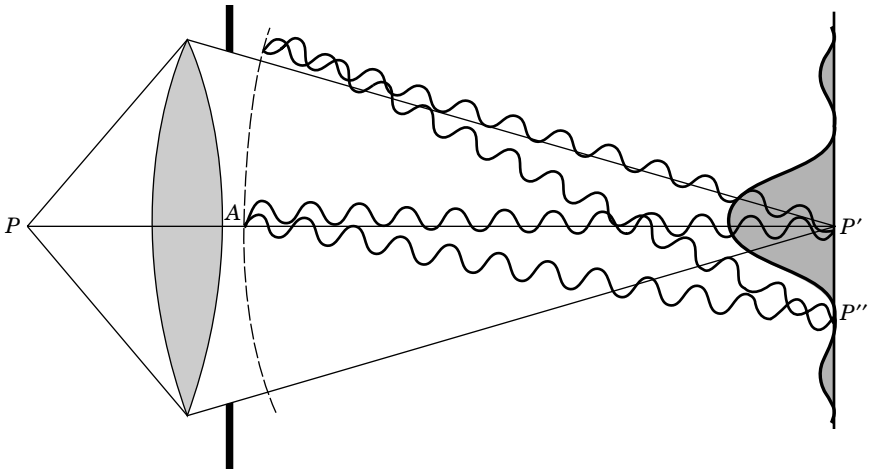

(a)

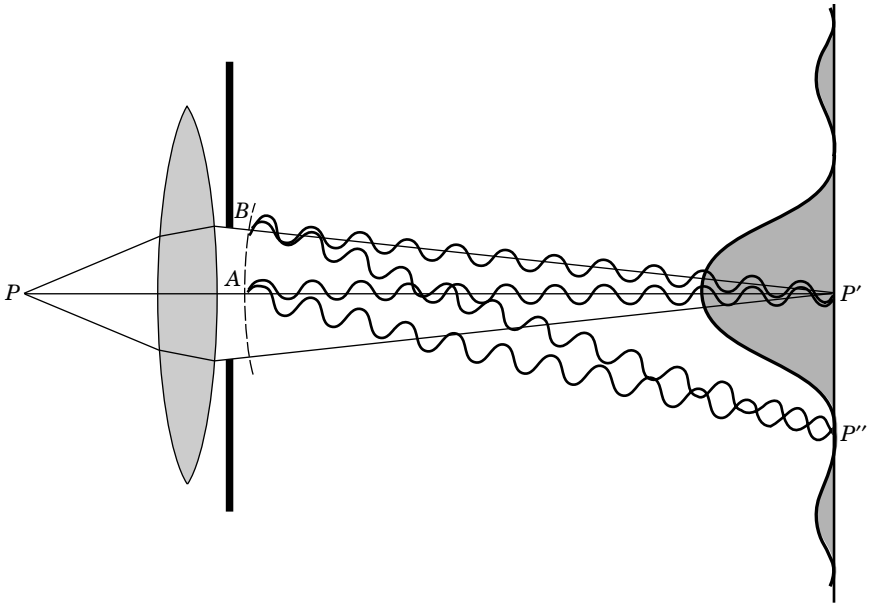

(b)

Figure 5-7

Aperture angle determines the size of the diffraction spot. Point source *P* and its conjugate image *P′* in the image plane. Point *P″* is moved laterally in the focal plane away from *P′* until destructive interference at a certain distance determines the location of the first diffraction minimum and thus the radius of the diffraction spot. (a) Points A and B in the wavefront with full lens aperture. (b) Points A and B in the wavefront with reduced aperture angle caused by partially stopping down the condenser iris diaphragm.

phase with each other and destructively interfere. The light intensity at this position (the first minimum in the diffraction pattern of the spot) is 0. Indeed, it can be shown that *the sum of contributions from all points in the aperture results in an amplitude of 0 at this location and nearly so at all other locations in the image plane other than in the central diffraction spot and surrounding diffraction rings.* A geometrical explanation of the phenomenon is given by Texereau (1963).

In Figure 5-7b we observe that the aperture (closing down the condenser diaphragm in a conjugate focal plane) reduces the angular aperture of the optical system, which increases the size of the diffraction spot and the distance $P'P''$ to the first diffraction minimum. Therefore, reducing the angular aperture decreases spatial resolution in the image. If we reexamine the optics of the pinhole camera, it now becomes clear why viewing a point source through a pinhole aperture held in front of the eye allows perception of an observable diffraction disk (Fig. 5-5). For the fully dilated eye the Airy disk of a point source covers ~2 cone cells on the retina, but with the reduced angular aperture using a pinhole, the disk diameter expands some 40-fold, stimulates dozens of receptor cells, and results in the perception of a disk.

DIFFRACTION BY A GRATING AND CALCULATION OF ITS LINE SPACING, *D*

We will now examine the diffraction of light at a specimen using a transparent diffraction grating as a model for demonstration and discussion. We should bear in mind that the principles of diffraction we observe at a grating on an optical bench resemble the phenomena that occur at specimens in the microscope. A *diffraction grating* is a planar substrate containing numerous parallel linear grooves or rulings, and like a biological specimen, light is strongly diffracted when the spacing between grooves is close to the wavelength of light (Fig. 5-8). If we illuminate the grating with a narrow beam from a monochromatic light source such as a laser pointer and project the diffracted light onto a screen 1 2 m distant, a bright, central 0th-order spot is observed, flanked by one or more higher-order diffraction spots, the 1st-, 2nd-, 3rd-, etc.-order diffraction maxima. The 0th-order spot is formed by waves that do not become diffracted during transmission through the grating. An imaginary line containing the diffraction spots on the screen is perpendicular to the orientation of rulings in the grating. The diffraction spots identify unique directions (diffraction angles) along which waves emitted from the grating are in the same phase and become reinforced as bright spots due to constructive interference. In the regions between the spots, the waves are out of phase and destructively interfere.

The *diffraction angle* θ of a grating is the angle subtended by the 0th- and 1st-order spots on the screen as seen from the grating (Fig. 5-9). The right triangle containing θ at the screen is congruent with another triangle at the grating defined by the wavelength of illumination, λ, and the spacing between rulings in the grating, d. Thus, $\sin\theta = \lambda/d$, and reinforcement of diffraction spots occurs at locations having an integral number of wavelengths that is, 1λ, 2λ, 3λ, and so on because diffracted rays arriving at these unique locations are in phase, have optical path lengths that differ by an integral number of wavelengths, and interfere constructively, giving bright diffraction spots. If $\sin\theta$ is calculated from the distance between diffraction spots on the screen and between the screen and the grating, the spacing d of the rulings in the grating can be determined using the *grating equation*

$$m\lambda = d\sin\theta,$$

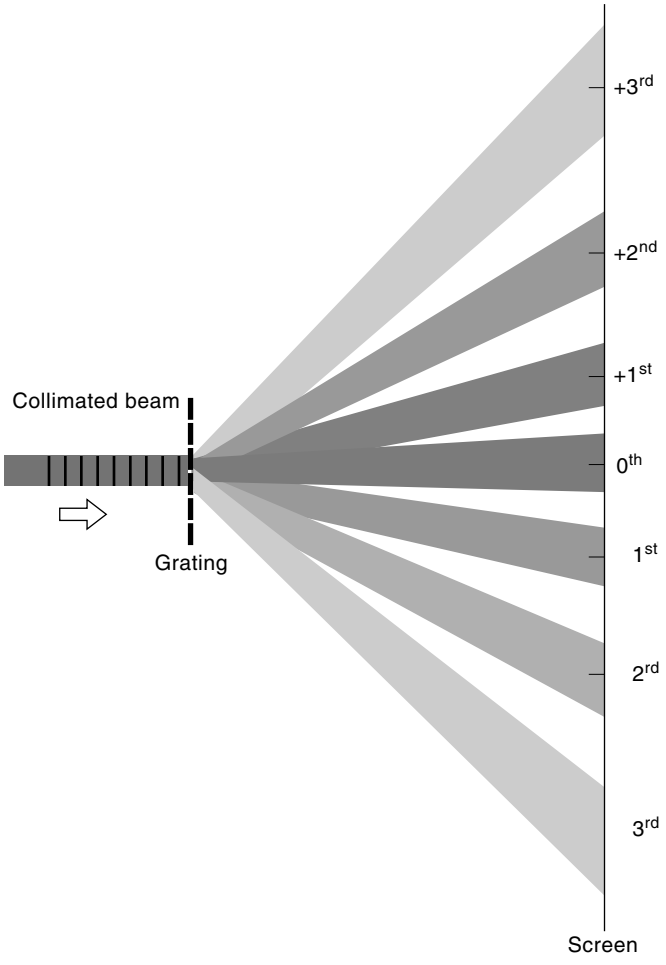

Figure 5-8
The action of a diffraction grating. Multiple orders of diffracted light are shown.

where λ is the wavelength and m is an integral number of diffraction spots. (For calculations based on the distance between the 1st- and 0th-order spots, $m = 1$; if the distance between the 2nd- and 0th-order spots is used, $m = 2$, etc.) Notice that the diffraction angle θ *increases* as the grating spacing d *decreases* and as the wavelength λ *increases.*

The effect of wavelength can be demonstrated by illuminating the grating with white light. Under this condition, the 0th-order spot appears white, while each higher-order diffraction spot appears as an elongated spectrum of colors. Thus, the diffraction angle depends directly on the wavelength. Blue light, being most energetic, is scattered the least, so the blue ends of the spectra are always located closest to the 0th-order central spot.

An alternate device, called *Hugyens principle,* can also be used to determine the location of the diffraction spots and diffraction angle θ of a grating. Christiaan Huygens, the Dutch physicist (1629 92), used a geometrical construction for determining the location of a propagating wavefront, now known as the *construction of Huygens wavelets* (Fig. 5-10). According to Huygens principle, every point on a propagating

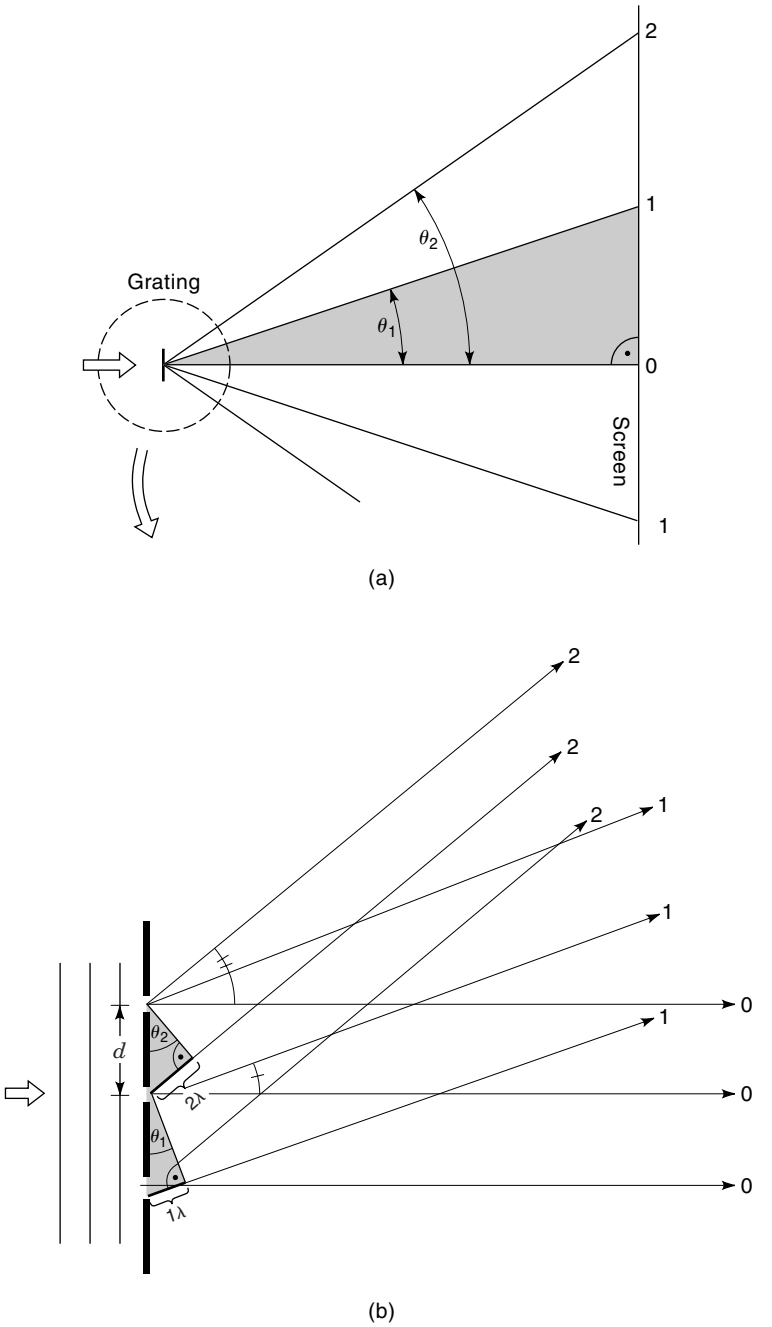

Figure 5-9

Dependence of scattering angle on grating spacing and wavelength. (a) Rays from a diffraction grating projected on a viewing screen. The angle of scattering of the 1st- and 2nd-order rays is shown as θ_1 and θ_2. The grating and 1st- and 2nd-order spots define a right triangle that includes θ_1 and is congruent with a triangle that can be delineated at the grating as shown in (b). (b) The diffracted rays at the grating define a right triangle that includes diffraction angle θ. For the 1st- and 2nd- etc.-order diffracted rays, the base of the triangle is an integral number of wavelengths, 1λ, 2 λ etc. Thus, the angle of diffraction depends on two parameters: the grating spacing *d* and wavelength λ.

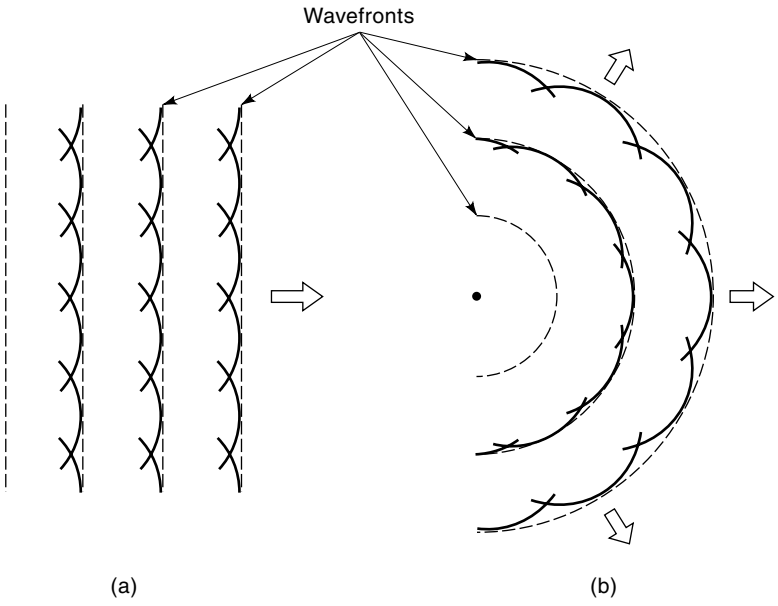

Figure 5-10
Huygens wavelets are used to describe the propagation of (a) planar and (b) spherical wavefronts.

wavefront serves as the source of *spherical secondary wavelets,* such that the wavefront at some later time is defined by the envelope covering these wavelets. Further, if wave propagation occurs in an isotropic medium, the secondary wavelets have the same frequency and velocity as the original reference wavefront. The geometrical construction of Huygens wavelets is a useful device for predicting the locations of wavefronts as modified by both refraction and diffraction; however, Huygens theory does not account for many wave-optical phenomena of diffraction, which require the application of newer approaches in physical optics.

When applied to the diffraction grating, we can use the construction of Huygens wavelets to determine the location of the diffraction spots and the diffraction angle. Take a moment to study the construction for a diffraction grating with spacing d in Figure 5-11, which emphasizes the concept that the diffraction spots occur at angles where the optical path lengths of constituent waves are an integral number of wavelengths λ. At locations between the diffraction spots, waves vary by a fraction of a wavelength and destructively interfere. Although Huygens wavelet construction accounts for the locations of diffraction spots, it does not account for all aspects of the diffraction process. For example, the sum of all of the energy present in the luminous regions of the diffraction pattern is known to equal the energy incident on the grating. This is inconsistent with ray particle models and predictions from the geometrical construction of wavelets that photons are distributed uniformly on the diffraction screen, being annihilated where there is destructive interference. We enter here a murky area where the wave and particle natures of light are difficult to reconcile.

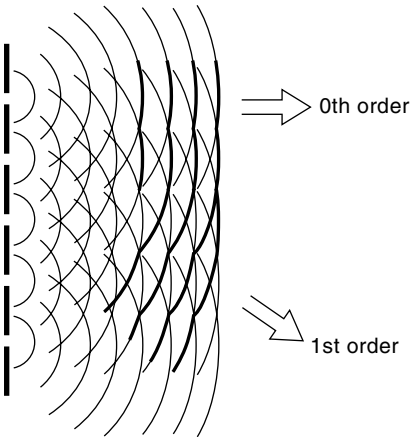

Figure 5-11
Geometrical determination of scattering angles in a diffraction grating using the construction of Huygens wavelets.

Demonstration: The Diffraction Grating

It is possible to see the trajectories of diffracted rays by immersing a transparent diffraction grating replica in a dish of water. Fill a 9 × 12 inch glass baking dish with water, add 1 2 mL of milk, and place the dish on a dark background. Place a small laser or laser pointer up against the dish and direct the beam at a diffraction grating immersed in the water. The rulings on the grating should be oriented vertically. The 0^{th}-order beam and higher order diffracted beams are made visible by the light-scattering properties of the miscelles of lipid and protein in the milk. Notice that the diffracted rays are linear and sharply defined. Each point along a ray represents a location where overlapping spherical wavefronts emergent from each illuminated diffracting ruling in the grating give constructive interference, meaning that the waves are in phase with one another, differing precisely by an integral number of wavelengths. The dark spaces in between the rays represent regions where the wavefronts are out of phase and give destructive interference. The geometry supporting destructive interference does not mean, however, that light self-annihilates in the dark zones. For any given point located in a dark zone, it can be seen that there is no visible light between the point and the illuminated spot on the grating. Instead, diffraction results in light energy being directed only along paths giving constructive interference. All of the light energy contained in the incident laser beam is contained in the 0^{th} order and higher order diffracted rays. The diffraction angle θ that is subtended at the grating by the 0^{th}-order ray and a higher order diffracted ray depends on the refractive index of the medium and on the wavelength, λ.

Illuminate a diffraction grating with a bright white light source and project the diffraction pattern on a wall or viewing screen (Fig. 5-12). It is convenient to use the I-beam optical bench so that the grating, filters, and masks can be stably mounted in holders clamped to the beam. If high-intensity xenon or mercury arc lamps are used, you should position a heat-absorbing filter (BG38 glass) or,

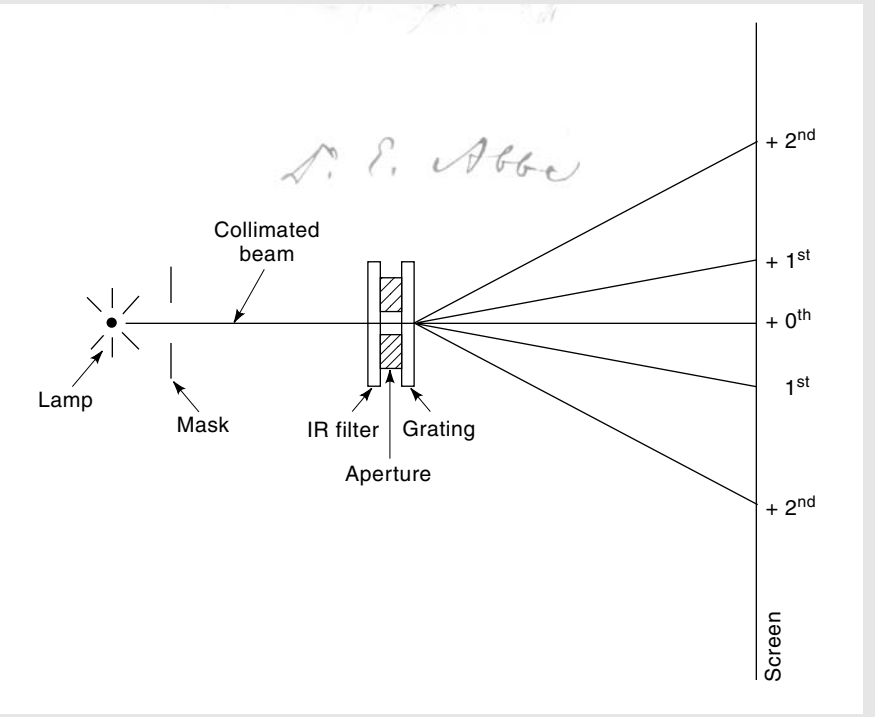

Figure 5-12

Demonstration of diffraction with a grating. An optical bench may be used to hold optical elements at fixed locations. A collimated bright white light source and a heat-cut filter are used to illuminate a diffraction grating covered by a closely apposed aperture mask containing a 2 3 mm hole or slit. If a slit is used instead of a hole, it should be perpendicular to the rulings in the grating.

better, a heat-reflecting mirror (hot mirror) between the lamp and the grating to keep the grating from melting. It is also useful to place an opaque metal mask (aluminum foil) containing a 3 4 mm diameter hole immediately in front of the grating in order to obtain a more sharply defined diffraction pattern.

On the viewing screen, notice the central 0th-order spot, white and very bright, flanked on two sides by 1st-, 2nd-, and higher-order diffraction spots, each of which appears as a bright spectrum of colors, with the blue ends of the spectra oriented toward the 0th-order spot. Higher-energy blue wavelengths are diffracted the least and are located closest to the 0th-order spot within each diffraction-order spectrum and in accordance with the relation already given, showing that the diffraction angle $\theta \propto \lambda/d$. It is easy to measure the angle θ by simple trigonometry, particularly when monochromatic light is used. When the grating is illuminated with monochromatic light from a laser pointer ($\lambda =$ 625 665 nm), all of the diffraction spots appear as sharply defined points.

Using a white card as a screen, move the card closer to the grating. Observe that the diffraction angle defined by the grating and the 1st- and 0th-order diffraction spots remains constant and that the spots move closer together as the card

approaches the grating. It is easy to see the linear diffracted rays by darkening the room and introducing a cloud of chalk or talcum dust between the grating and the screen.

Finally, examine the diffraction pattern of a sinusoidal (holographic) grating. The sinusoidal grating channels much of the incident light into the 1st-order diffraction spots, which are much brighter than the spots produced by a conventional ruled grating. Such gratings are very useful for examining the spectra of filters and illuminators.

ABBE S THEORY FOR IMAGE FORMATION IN THE MICROSCOPE

Ernst Abbe (1840 1905) developed the theory for image formation in the light microscope while working in the Carl Zeiss optical workshop in Jena, Germany (Fig. 5-13). Abbe observed that diffracted light from a periodic specimen produces a diffraction pattern of the object in the back focal plane (the diffraction plane) of the objective lens. *According to Abbe s theory, interference between 0th- and higher-order diffracted rays in the image plane generates image contrast and determines the limit of spatial resolution that can be provided by an objective.* For a periodic object such as a diffraction grating, it is easy to demonstrate that light from at least two orders of diffraction must be captured by the objective in order to form an image (see Exercise, this Chapter). In the minimal case, this could include light coming from two adjacent diffraction spots, such as the 0th- and one 1st-order spot generated by the grating. If light from only a single diffraction order is collected by the lens (only the 0th order is collected), there is no interference, and no image is formed. Put another way, there is no image if light diffracted at the specimen is excluded from the lens. Extending the concept further, the larger the number of diffraction orders collected by the objective, the sharper and better resolved (the greater the information content) are the details in the image.

Objects that exhibit fine, periodic details (diffraction gratings, diatoms, striated muscle) provide important insights about the roles of diffraction and interference in image formation. Figure 5-14 shows a diffraction grating with periodic rulings illuminated by a collimated beam of light having planar wavefronts. Light diffracted by the rulings is collected by a lens, and an image of the rulings is created in the primary image plane.

Note the following:

A certain amount of incident light does not interact with the specimen and is transmitted as undeviated (nondiffracted) rays. These rays form the central 0th-order diffraction spot in the diffraction plane and go on to evenly illuminate the entire image plane.

Each ruling in the grating acts as an independent source of diffracted waves that radiate outward as a series of spherical wavefronts (Huygens wavelets) toward the objective lens. Note that the aperture of the lens is large enough to capture some of the diffracted light. The effective NA of the objective is critically dependent on the setting of the condenser aperture. The diffracted light forms higher-order diffraction spots flanking the 0th-order spot in the diffraction plane.

The 0th- and higher-order diffraction spots in the diffraction plane correspond to locations where there is constructive interference of waves that differ in their path

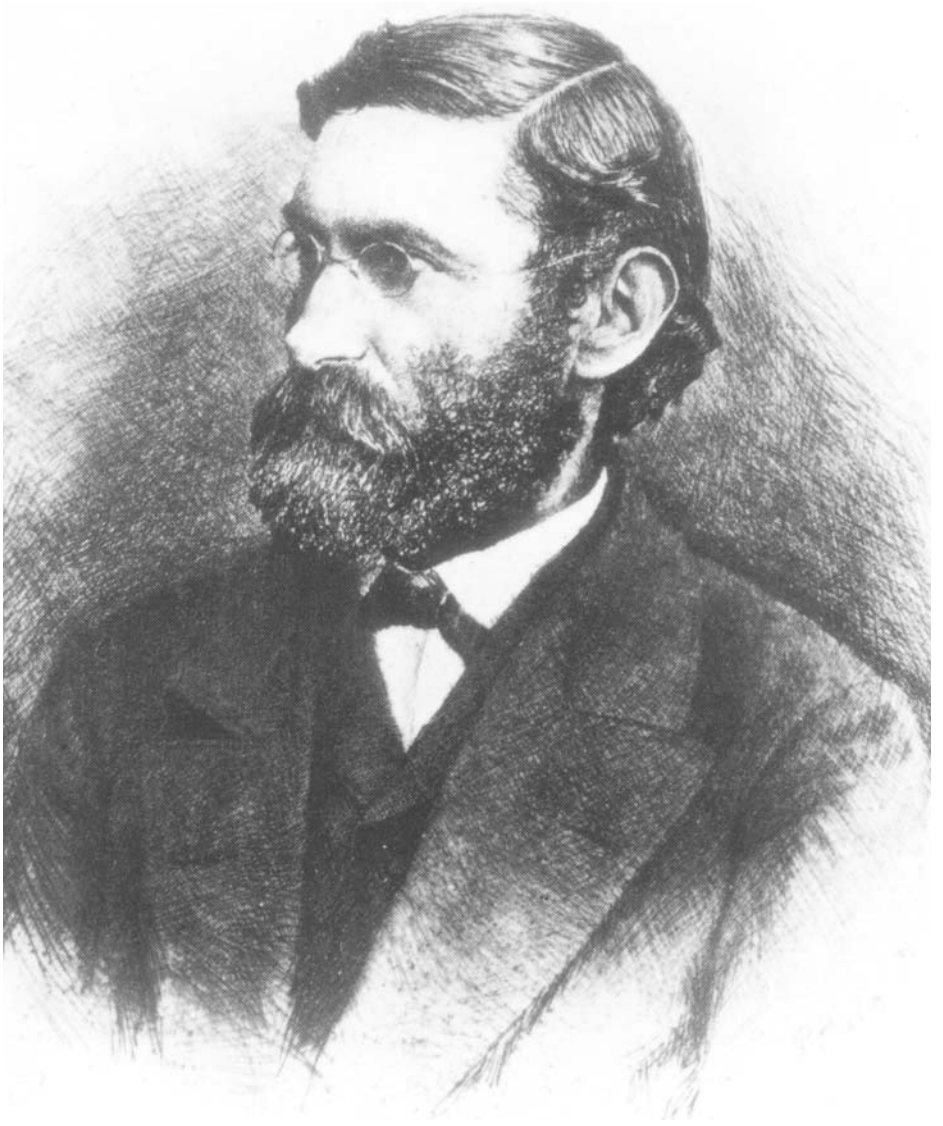

Figure 5-13

Ernst Abbe, 1840 1905. Principles of microscope and objective lens design, the theory of image formation in the microscope, and standardized lens manufacturing procedures all trace their beginnings to the work of Ernst Abbe and his collaborations with Carl Zeiss in Jena, Germany, in the 1860s. Until then, lens making was an art and a craft, but the new industrial philosophy demanded technical perfection, lens designs based on theory and research, and improvements in raw materials. At Abbe s initiative, lens curvatures were examined using an interference test with Newton s rings, and lens designs were based on Abbe s sine-squared condition to remove aberrations. He created the first planachromatic lens, and after much research, the apochromatic lens, which was commercially sold in 1886. After many false starts over a 20-year period, the research-theory-testing approach for manufacturing lenses proved to be successful. These improvements and new photographic lens designs required new types of glass with values of refractive index and color dispersion that were not then available. Abbe and Zeiss won grants and developed new glasses in collaborations with the industrialist, Otto Schott, owner of the Jena Glassworks. Other

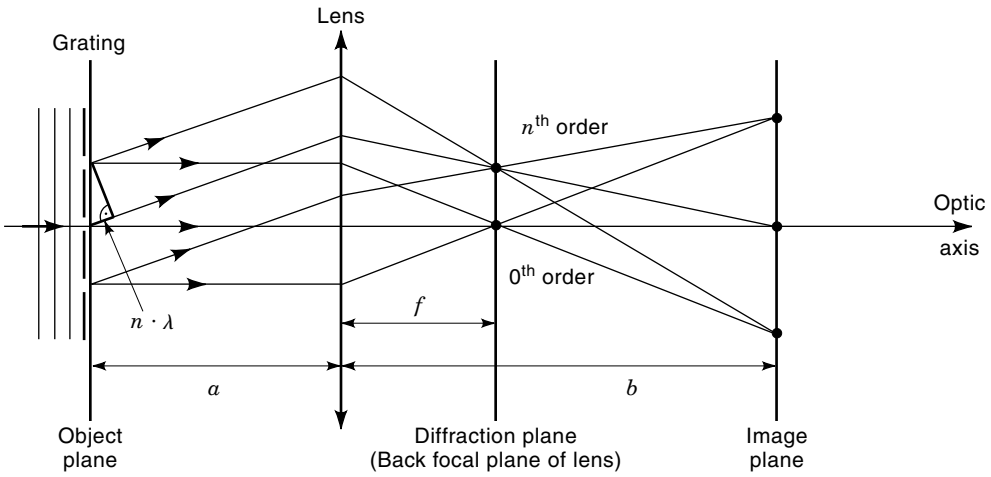

Figure 5-14

Abbe s theory for image formation in a light microscope. An objective lens focused on a grating ($2f > a > f$) in the object plane produces a magnified real image of the grating in the image plane. The diffraction plane is located at 1f in the back aperture of the lens. An incident planar wavefront is shown. Diffracted nth-order and nondiffracted 0th-order rays are separated in the diffraction plane, but are combined in the image plane.

lengths by exactly 1, 2, 3, . . . wavelengths, respectively. The waves at each spot are exactly in phase and are diffracted at the slits in the specimen at the same unique angle of diffraction (θ). Note that each point in the diffraction plane corresponds to a certain angle of light leaving the specimen. The absence of light between the spots is due to interference between waves that are in or out of phase with each other. The 0th- and higher-order diffraction spots are most clearly focused and separated from one another in the diffraction plane (the rear focal plane of the objective lens).

Image formation in the image plane is due to the interference of undeviated and deviated components that are now rejoined and interfere in the image plane, causing the resultant waves in the image plane to vary in amplitude and generate contrast. Abbe demonstrated that at least two different orders of light must be captured by a lens for interference to occur in the image plane (Fig. 5-15).

---

inventions were the Abbe achromatic condenser, compensating eyepieces for removing residual color aberration, and many other significant items of optical testing equipment. Abbe is perhaps most famous for his extensive research on microscope image formation and his diffraction theory, which was published in 1873 and 1877. Using a diffraction grating, he demonstrated that image formation requires the collection of diffracted specimen rays by the objective lens and interference of these rays in the image plane. By manipulating the diffraction pattern in the back aperture, he could affect the appearance of the image. Abbe s theory has been summarized as follows: *The microscope image is the interference effect of a diffraction phenomenon.* Abbe also introduced the concept of numerical aperture ($n \sin\theta$) and demonstrated the importance of angular aperture on spatial resolution. It took 50 years for his theory to become universally accepted, and it has remained the foundation of microscope optical theory ever since. Ernst Abbe was also a quiet but active social reformer. At the Zeiss Optical Works, he introduced unheard-of reforms, including the 8-hour day, sick benefits, and paid vacations. Upon his death, the company was handed over to the Carl Zeiss Foundation, of which the workers were part owners.

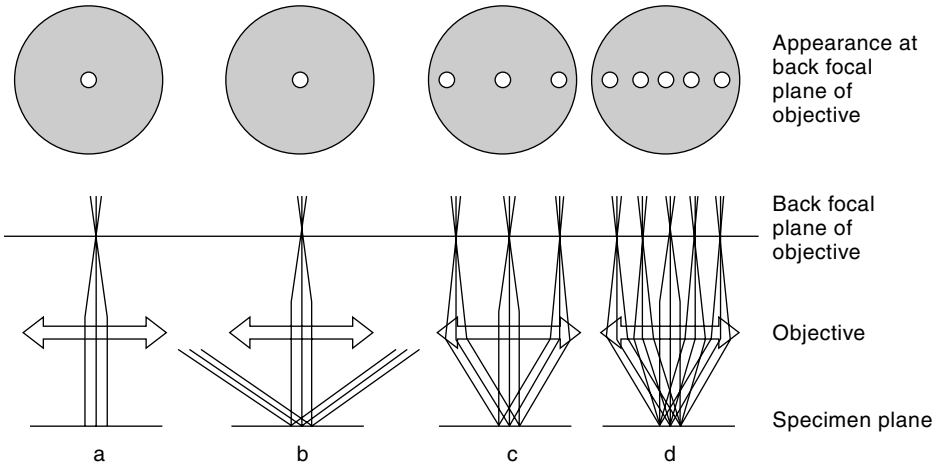

Figure 5-15

Generation of an image by interference requires collection of two adjacent orders of diffracted light by the objective lens. If diffraction at the specimen does not occur (a), or diffracted rays are not collected by the objective (b), no image is formed. In (c), a minimum of two adjacent diffraction orders (0th and 1st) are collected, and an image is formed. In (d), multiple diffracted orders are collected, leading to a high degree of definition in the image.

A periodic specimen with an interperiod spacing d gives rise to a periodic pattern with spacing D in the diffraction plane, where $D \sim 1/d$. Therefore, the smaller the spacings in the object, the farther apart the spots are in the diffraction plane, and vice versa. The relationship is

$$d \approx f\lambda/D \cos\theta$$

where f is the focal length of the lens, λ is the wavelength, and θ is the acute angle at the principal plane in the objective lens from which the focal length is measured and which forms a right triangle together with the 0th- and 1st-order diffraction spots.

Abbe s theory of image formation explains the following important points: If a specimen does not diffract light or if the objective does not capture the diffracted light from an object, no image is formed in the image plane. If portions of two adjacent orders are captured, an image is formed, but the image may be barely resolved and indistinct. If multiple orders of diffracted light are captured, a sharply defined image is formed. The theory is also the basis for determining the spatial resolution of the light microscope, which is the subject of the next chapter.

DIFFRACTION PATTERN FORMATION IN THE BACK APERTURE OF THE OBJECTIVE LENS

Let us now consider the diffraction pattern in the microscope s diffraction plane in the back aperture (back focal plane) of the objective lens. Under conditions of Koehler illumination, a diffraction image of a specimen is formed just behind the objective in the

objective s back (or rear) focal plane. You should take a moment to reinspect the figures in Chapter 1 and recall that this plane is conjugate with other aperture planes in the microscope that is, the lamp filament, the front focal plane of the condenser, and the iris aperture of the eye. For specimens having periodic details (a diffraction grating) and under certain conditions of diaphragm adjustments, you can inspect the diffraction pattern of an object using a Bertrand lens. The diffraction pattern in the back aperture and the image in the image plane are called *inverse transforms of each other,* since distance relations among objects seen in one plane are *reciprocally* related to spacings present in the other plane, as will now be explained.

Demonstration: Observing the Diffraction Image in the Back Focal Plane of a Lens.

It is easy to confirm the presence of a diffraction image of an object in the back aperture of a lens using an I-beam optical bench, a 3 mW HeNe laser light source, and an electron microscope copper grid (Figure 5-16). A 50 mm or shorter focal length lens is placed just in front of the laser to spread the beam so as to illuminate the full diameter of the grid. The EM grid taped to a glass microscope slide and mounted on a lens holder serves as an object. Position the grid at a distance that allows full illumination of its surface by the laser. Confirm that the grid generates a diffraction pattern by inserting a piece of paper into the beam at various locations behind the grid. Now position an optical bench demonstration lens of 50 100 mm focal length just over 1 focal length from the grid to create a sharply focused image (real intermediate image) of the grid on a projection screen some 2 3 meters away from the lens. Adjust the lens position as required to obtain a focused image of the grid on the screen. The image reveals an orthogonal pattern of square empty holes delimited by metal bars of the grid, which is a stamped piece of copper foil. To see the focused diffraction pattern of the grid, insert a white sheet of paper in the optical path at one focal length away from the lens. The diffraction pattern consists of an orthogonal pattern of bright points of light (see Fig. 5-1). Confirm that the focused diffraction image is located precisely in the back focal plane at 1 focal length distance by moving the paper screen back and forth along the beam.

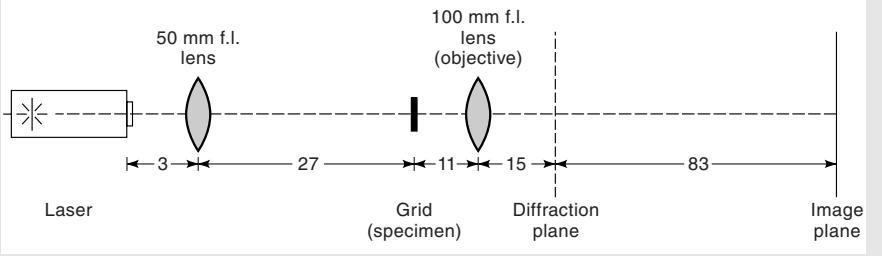

Figure 5-16

Demonstration of the diffraction image in the back focal plane of a lens.

Let us first consider the image of an object such as a diffraction grating with lines spaced just a few micrometers or less apart. Light that passes through the grating (we might imagine any microscope specimen) and does not interact with it is called direct light and forms a small central spot (the 0th-order diffraction spot) in the middle of the diffraction pattern. Light that becomes diffracted (diffracted waves) forms a pattern of widely separated 1st-, 2nd-, 3rd-, etc.-order spots flanking the 0th-order spot. The diffraction patterns of periodic objects such as diatoms or striated muscle can be observed by closing the condenser diaphragm down to a minimum and inspecting the diffraction plane with a Bertrand lens. It is understood that the light contained in the diffraction pattern goes on to form the image of the grating through interference in the real intermediate image plane in the eyepieces of the microscope. Looking at the image through the eyepieces, we do not see the diffraction pattern, but the inverse transform that is derived from it. Thus, we say that the *object image is the inverse transform of the diffraction pattern in the back aperture.* The reciprocal nature of the space relationships of the two images is described as follows: Fine periodic features separated by short distances in the object and image are seen as widely separated diffraction spots in the diffraction image; coarse features separated by relatively long distances in the object and real intermediate image take the form of closely separated diffraction spots close to the central 0th-order spot in the diffraction pattern.

Joseph Gall demonstrated this relationship by placing a transparent image (photographic negative) of a periodic polymer at the back aperture and by providing illumination from a pinhole placed at the lamp s field stop. There was no specimen on the stage of the microscope. Looking in the eyepieces, the diffraction pattern (the inverse transform) of the polymer is observed. Used this way, the microscope functions as an optical diffractometer (Gall, 1967). Thus, images located in the diffraction plane and in the image plane are inverse transforms of one another, and the two images exhibit space relationships that are related as the reciprocal of the space relations in the other image. The exercise at the end of this chapter reinforces these points. We will revisit this concept throughout the book, particularly in the chapters on phase contrast microscopy and in the section on fast Fourier transforms in Chapter 15.

PRESERVATION OF COHERENCE: AN ESSENTIAL REQUIREMENT FOR IMAGE FORMATION

Our discussion of the role of diffraction and interference in image formation would not be complete without considering the requirement for coherent light in the microscope. Object illumination with rays that are partially coherent is required for all forms of interference light microscopy (phase contrast, polarization, differential interference contrast) discussed in the following chapters.

Nearly all incoherent light sources, even incandescent filament lamps, are partially coherent that is, the waves (wave bundle) comprising each minute ray emanating from a point on the filament vibrate in phase with each other. In reality, the degree of coherence within a given ray is only partial, since the photons vibrate slightly out of phase with each other. The distance over which the waves exhibit strong coherence is also limited just a few dozen wavelengths or so so that if you examined the amplitude of the ray along its length, you would see it alternate between high-amplitude states, where the waves vibrate coherently, and low-amplitude states, where waves are transiently out of phase with each other. In contrast, laser beams can be coherent over

meters of distance, whereas waves emitted from a fluorescence source are completely incoherent.

The cause of coherence derives from the fact that atoms in a microscopic domain in the filament, excited to the point that they emit photons, mutually influence each other, which leads to synchronous photon emission. Thus, a tungsten filament or the ionized plasma in a mercury arc may each be considered as a large collection of minute atomic neighborhoods, each synchronously emitting photons. A discrete number of coherent waves following the same trajectory is thus called a ray or pencil of light. The action of the collector lens of the illuminator is to form an image of the filament in the front aperture of the condenser, which then becomes the source of partially coherent rays that illuminate the object in the specimen plane (Fig. 5-17).

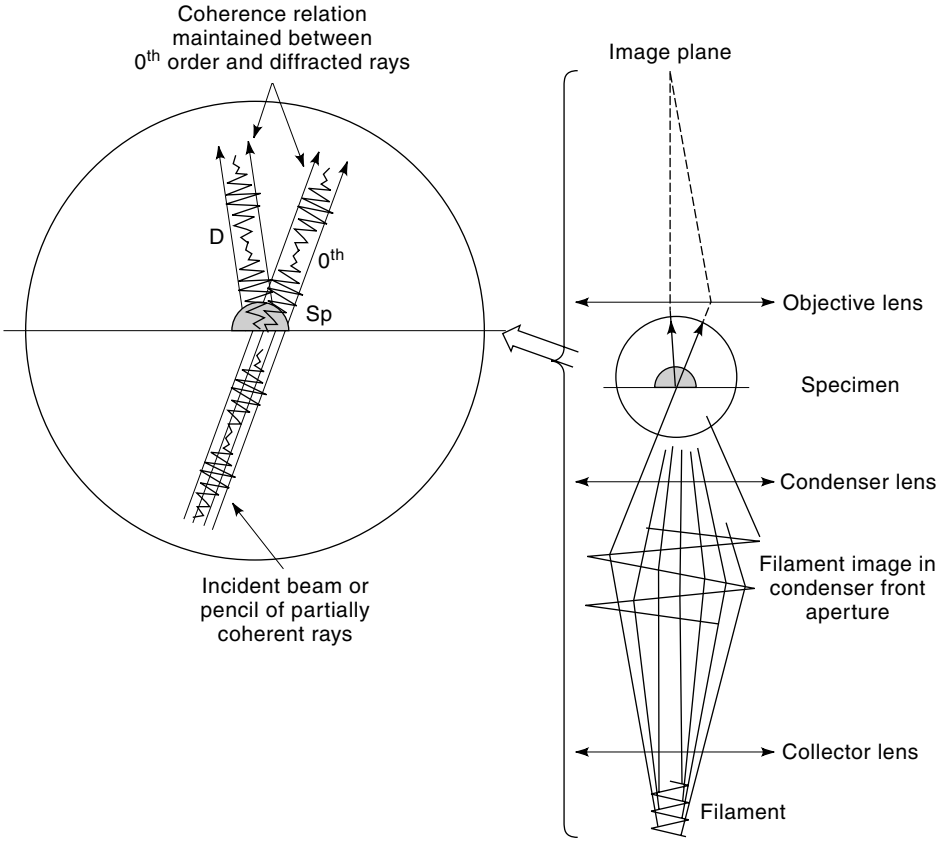

Figure 5-17

Partially coherent wave bundles in the light microscope. Small domains in the lamp filament emit partially coherent wave bundles that reform the image of the filament in the front aperture of the condenser. Rays (small beams or pencils of partially coherent photons) incident on a small particle in the specimen plane are broken up into diffracted and undeviated (0th-order) waves that maintain their coherence relationship. A myriad of ray pairs go on through the objective lens and combine incoherently with other rays in the image plane to form the image. The coherence relationship between undeviated and diffracted rays is essential for image formation in all forms of interference microscopy (phase contrast, polarization, differential interference) described in the following chapters.

For a given ray incident at an object, it is now possible to see that a coherence relationship exists between the diffracted and undiffracted (0th-order) beams. This coherence relationship is maintained between the object and the image plane, where waves recombine and interfere. At that site, the myriad coherent wave partners add incoherently with other waves to produce the final image. This important concept underlies many forms of light microscopy.

Exercise: Diffraction by Microscope Specimens

Determine the periodicity of unknown diffraction gratings using the diffraction equation, $m\lambda = d \sin\theta$. Measure the distances in centimeters between the 1st- and 0th-order spots on a projection screen and the distance between one of the spots and the grating to calculate $\sin\theta$ and the grating spacing, d. It is easiest to perform this measurement using a narrow, monochromatic beam such as that provided by a laser pointer.

Review Koehler illumination and check the focus of the illuminator of your microscope. Focus on a piece of diffraction grating mounted on a glass microscope slide with a 40× dry objective, and calculate the spacing using the eyepiece reticule and calibration factor determined in the exercise for Chapter 1. For accuracy, measure the number of eyepiece units covering 10 or more spacings on the stage micrometer, repeat the procedure 10 times, and determine the mean value. How well do the two numbers agree?

Examine and compare the diffraction patterns of various other specimens on the projection screen and estimate their periods (suggestions: microscopic barbules on a bird feather, grooves on a semitransparent CD disk). If the CD is completely opaque, treat it as a reflection grating, tilting the CD at a 45° angle to form a right triangle between the 0th-order spot, the CD, and the light source using the equation for a 90° reflection: $d = \sqrt{2}\lambda/\sin\theta$. Use the laser pointer as a light source.

Focus the grating in monochromatic green light using a 10× objective with your microscope, stop down (maximally constrict) the condenser aperture diaphragm, and look to see if you can still resolve the grating in normal viewing mode. Examine the diffraction pattern of the grating with an eyepiece telescope under conditions where the image is not resolved, barely resolved, and fully resolved. Do you agree with Abbe s conclusion that a minimum of two adjacent diffraction orders is required for resolution?

Using the same condenser position, remove the green filter and examine the grating in red and blue light. For each color filter, examine the pattern of diffraction spots with the eyepiece telescope and note the corresponding changes in the spacing between the 1st-order diffraction spots. Do your observations agree with the relationship between spatial resolution and wavelength?

CHAPTER

6

DIFFRACTION AND SPATIAL RESOLUTION

OVERVIEW

In this chapter we examine the role of diffraction in determining spatial resolution and image contrast in the light microscope. In the previous chapter we emphasized that Abbe s theory of image formation in the light microscope is based on three fundamental actions: diffraction of light by the specimen, collection of diffracted rays by the objective, and interference of diffracted and nondiffracted rays in the image plane. The key element in the microscope s imaging system is the objective lens, which determines the precision with which these actions are effected. As an example, examine the remarkable resolution and contrast in the image of the diatom, *Pleurosigma,* made with an apochromatic objective designed by Abbe and introduced by Carl Zeiss over 100 years ago (Fig. 6-1). To understand how such high-resolution images are obtained, we examine an important parameter of the objective, the numerical aperture, the angle over which the objective can collect diffracted rays from the specimen and the key parameter determining spatial resolution. We also investigate the effect of numerical aperture on image contrast. In examining the requirements for optimizing resolution and contrast, we make an unsettling discovery: It is impossible to obtain maximal spatial resolution and optimal contrast using a single microscope setting. A compromise is required that forces us to give up some spatial resolution in return for an acceptable level of contrast.

NUMERICAL APERTURE

Implicit in the Overview is an understanding that the objective aperture must capture some of the diffracted rays from the specimen in order to form an image, and that lenses that can capture light over a wide angle should give better resolution than an objective that collects light over a narrower angle. In the light microscope, the angular aperture is described in terms of the *numerical aperture* (NA) as

$$\mathrm{NA} = n \sin\theta,$$

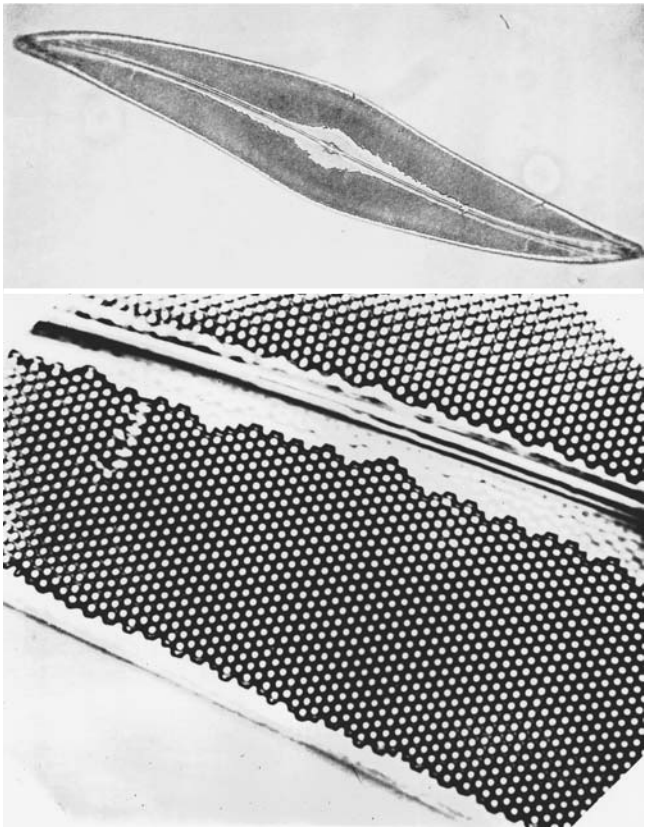

Figure 6-1
Resolution of the pores in a diatom shell with an apochromatic objective lens. Joseph Gall described these historic photographs of the diatom *Pleurosigma* prepared over 100 years ago using one of Abbe s lenses (*Molecular Biology of the Cell,* vol. 4, no. 10, 1993). The photographs . . . are taken from a Zeiss catalog published in 1888 in which Abbe s apochromatic objectives were advertised. Both figures show the silica shell of the diatom *Pleurosigma angulatum.* Because of the regular patterns of minute holes in their shells, diatoms have long been favorite objects for testing the resolution of microscope objectives. The top figure shows an entire shell at 500×, a magnification beyond which many 19th-century objectives would show little additional detail. The bottom figure, reproduced here and in the original catalog at a remarkable 4900×, was made with an apochromatic oil immersion objective of 2.0 mm focal length and a numerical aperture of 1.3. The center-to-center spacing of the holes in the shell is 0.65 μm, and the diameter of the holes themselves is about 0.40 μm. Almost certainly this objective resolved down to its theoretical limit of 0.26 μm in green light.

where θ is the half angle of the cone of specimen light accepted by the objective lens and n is the refractive index of the medium between the lens and the specimen. For dry lenses used in air, $n = 1$; for oil immersion objectives, $n = 1.515$.

The diffraction angles capable of being accepted by dry and oil immersion objective lenses are compared in Figure 6-2. By increasing the refractive index of the medium between the lens and coverslip, the angle of diffracted rays collected by the objective is increased. Because immersion oil has the same refractive index as the glass coverslip

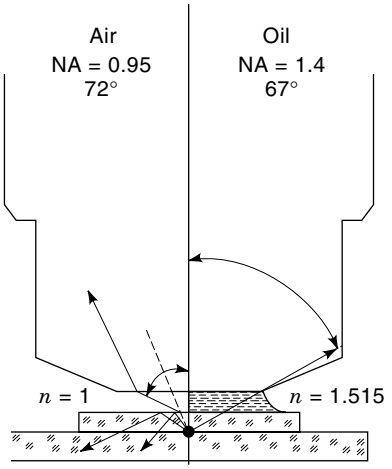

Figure 6-2

Effect of immersion oil on increasing the angular extent over which diffracted rays can be accepted by an objective lens. Numerical aperture is directly dependent on the wavelength λ and the sine of the half angle of the cone of illumination θ accepted by the front lens of the objective. For dry lenses, NA is limited, because rays subtending angles of 41° or greater are lost by total internal reflection and never enter the lens (dotted line). The practical limit for a dry lens is ~39°, which corresponds to an acceptance angle of 72°, and an NA of 0.95. By adding high-refractive index immersion oil matching that of the glass coverslip ($n = 1.515$), an oil immersion objective can collect light diffracted up to 67°, which corresponds to NA = 1.4.

(1.515), refraction of specimen rays at the coverslip-air interface is eliminated, the effective half angle is increased, and resolution is improved. The reader can refer to Pluta (1988) for more details on this important phenomenon.

SPATIAL RESOLUTION

For point objects that are self-luminous (fluorescence microscopy, dark-field microscopy), or for nonluminous points that are examined by bright-field microscopy in transmitted light where the condenser NA is ≥ the objective NA, the *resolving power* of the microscope is defined as

$$d = 0.61\lambda/\text{NA},$$

where d is the minimum resolved distance in μm, λ is the wavelength in μm, and NA is the numerical aperture of the objective lens.

In the case of bright-field microscopy, where the condenser NA < objective NA (the condenser aperture is closed down and/or an oil immersion condenser is used in the absence of oil), the resolution is given as

$$d = \frac{1.22\lambda}{\text{condenser NA} + \text{objective NA}}.$$

These equations describe the *Rayleigh criterion* for the resolution of two closely spaced diffraction spots in the image plane. By this criterion, *two adjacent object points are defined as being resolved when the central diffraction spot (Airy disk) of one point coincides with the first diffraction minimum of the other point in the image plane* (Fig. 6-3). The condition of being resolved assumes that the image is projected on the retina or detector with adequate magnification. Recording the real intermediate image on film or viewing the image in the microscope with a typical 10× eyepiece is usually adequate, but detectors for electronic imaging require special consideration (discussed in Chapters 12, 13, and 14). The Rayleigh resolution limit pertains to two luminous points in a dark field or to objects illuminated by incoherent light. For a condenser and objective with NA = 1.3 and using monochromatic light at 546 nm under conditions of oil immersion, the limit of spatial resolution $d = 0.61\lambda/\text{NA} = 0.26$ μm. Numerical apertures are engraved on the lens cap of the condenser and the barrel of the objective lens.

An image of an extended object consists of a pattern of overlapping diffraction spots, the location of every point x,y in the object corresponding to the center of a diffraction spot x,y in the image. Imagine for a moment a specimen consisting of a crowded field of submicroscopic particles (point objects). For a given objective magni-

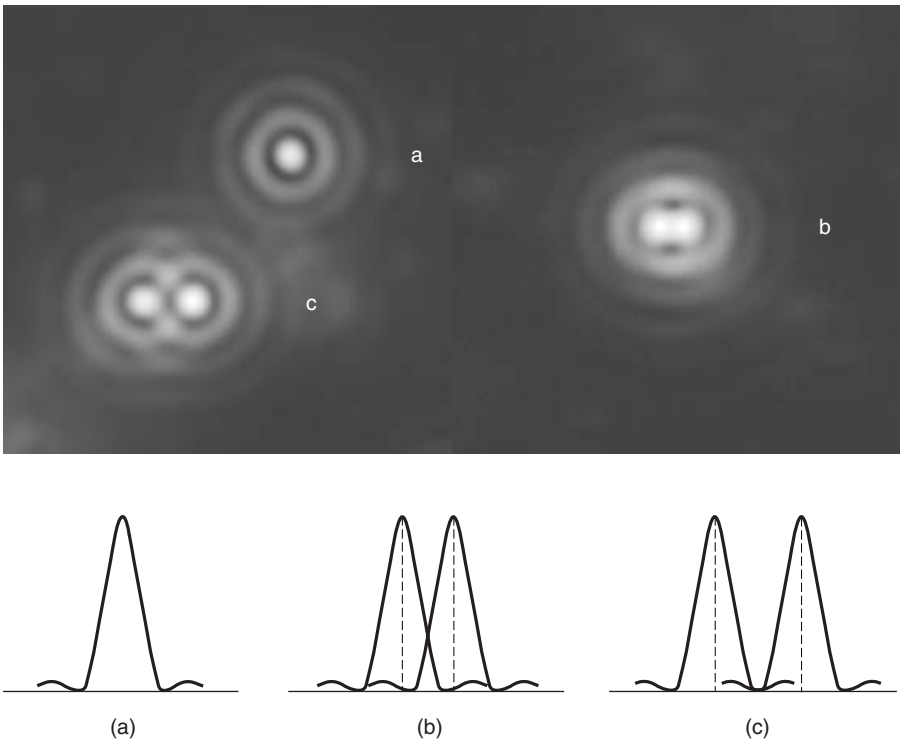

Figure 6-3

Rayleigh criterion for spatial resolution. (a) Profile of a single diffraction pattern: The bright Airy disk and 1st- and 2nd-order diffraction rings are visible. (b) Profile of two disks separated at the Rayleigh limit such that the maximum of a disk overlaps the first minimum of the other disk: The points are now just barely resolved. (c) Profile of two disks at a separation distance such that the maximum of each disk overlaps the second minimum of the other disk: The points are clearly resolved.

fication, if the angular aperture of a microscope is increased, as occurs when opening the condenser diaphragm or when changing the objective for one with the same magnification but a higher NA, the diffraction spots in the image grow smaller and the image is better resolved (Fig. 6-4). Thus, larger aperture angles allow diffracted rays to be included in the objective, permitting resolution of specimen detail that otherwise might not be resolved (Fig. 6-5).

The optical limit of spatial resolution is important for interpreting microscope images. Irregularities in the shapes of particles greater than the limiting size (0.52 μm diameter in the example cited previously) just begin to be resolved, but particles smaller than this limit appear as circular diffraction disks, and, regardless of their true sizes and shapes, always have the same apparent diameter of 0.52 μm. (The apparent variability in the sizes of subresolution particles is due to variations in their intensities, not to variability in the size of their diffraction spots.) Thus, whereas minute organelles and filaments such as microtubules can be *detected* in the light microscope, their apparent diameter (for the lens given previously) is always 0.52 μm, and their true diameters are *not resolved.* It should therefore be apparent that two minute objects whose center-to-center distance is less than 0.26 μm cannot be resolved, but that two objects with physical radii smaller than this size can easily be resolved from each other if they are farther apart than 0.26 μm.

It must be remembered that *adjusting the condenser aperture directly affects spatial resolution in the microscope.* Since a large aperture angle is required for maximum resolution, the front aperture of the condenser must be fully illuminated. Stopping down

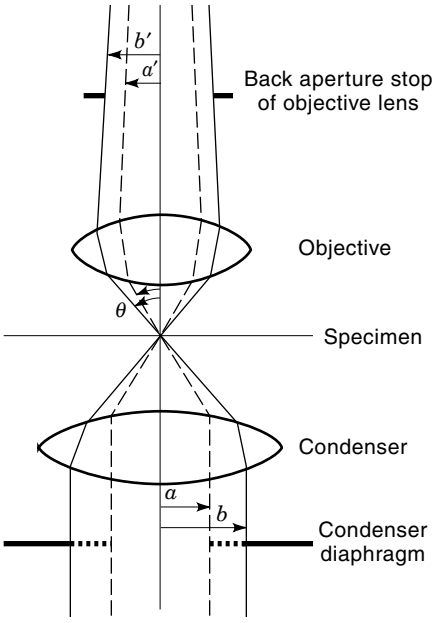

Figure 6-4

Role of the condenser diaphragm in determining the effective numerical aperture. Closing the front aperture diaphragm of the condenser from position *b* to *a* limits the angle θ of the illumination cone reaching the objective, and thus the effective numerical aperture. Notice that the back aperture of the objective is no longer filled at the reduced setting.

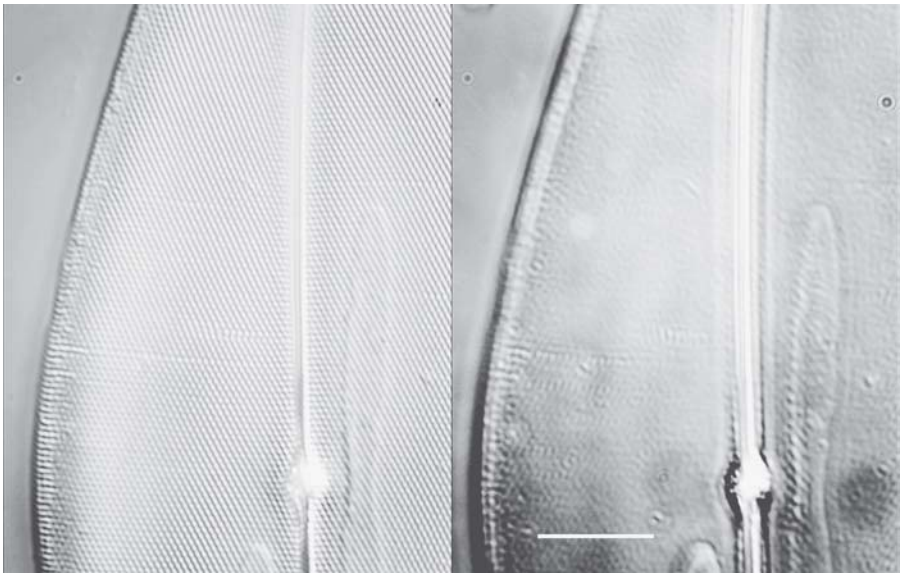

Figure 6-5

Effect of numerical aperture on spatial resolution. The diatom *Pleurosigma* photographed with a 25×, 0.8 NA oil immersion lens using DIC optics. (a) Condenser aperture open, showing the near hexagonal pattern of pores. (b) The same object with the condenser diaphragm closed. The 1st-order diffracted rays from the pores are not captured by the objective with a narrow cone of illumination. Spatial resolution is reduced, and the pores are not resolved. Bar = 10 μm.

the condenser diaphragm limits the number of higher-order diffracted rays that can be included in the objective and reduces resolution. In an extreme case, the condenser aperture may be nearly closed in a mistaken effort to reduce light intensity. Then the half angle of the light cone entering the lens is greatly restricted, and resolution in the image is reduced significantly. The proper way to reduce light intensity is to turn down the voltage supply of the lamp or insert neutral density filters to attenuate the illumination.

DEPTH OF FIELD AND DEPTH OF FOCUS

Just as diffraction and the wave nature of light determine that the image of a point object is a diffraction disk of finite diameter, so do the same laws determine that the disk has a measurable thickness along the z-axis. *Depth of field Z* in the object plane refers to the thickness of the optical section along the z-axis within which objects in the specimen are in focus; *depth of focus* is the thickness of the image plane itself. Our present comments are directed to the depth of field. For diffraction-limited optics, the wave-optical value of Z is given as

$$Z = n\lambda/\mathrm{NA}^2,$$

where n is the refractive index of the medium between the lens and the object, λ is the wavelength of light in air, and NA is the numerical aperture of the objective lens. Thus,

the larger the aperture angle (the higher the NA), the shallower will be the depth of field. The concept of depth of field is vivid in the minds of all of those who use cameras. Short-focal-length (fast) lenses with small focal ratios ($<f/4$) have a shallow depth of field, whereas the depth of field of long-focal-length (slow) lenses ($>f/16$) is relatively deep. At one extreme is the pinhole camera, which has an infinitely small NA and an infinite depth of field all objects, both near and far, are simultaneously in focus in such a camera.

The depth of field along the z-axis is determined by several contributing factors, including principles of geometrical and physical optics, lens aberrations, the degree of physiological accommodation by the eye, and overall magnification. These variables and quantitative solutions for each are described in detail by Berek (1927), and are reviewed by Inoué (in Pawley, 1995) and Pluta (1988). Calculated values of the wave optical depth of field for a variety of objective lenses are given in Table 4-1.

The depth of field for a particular objective can be measured quickly and unambiguously using the microscope. A planar periodic specimen such as a diffraction grating is mounted obliquely on a specimen slide by propping up one end of the grating using the edge of a coverslip of known thickness. When the grating is examined in the microscope, it will be seen that only a narrow zone of grating will be in focus at any particular setting of the specimen focus dial. The depth of field z is then calculated from the width w of the focused zone (obtained photographically) and the angle of tilt α of the grating through the relationship

$$Z = nw \tan\alpha,$$

where n is the refractive index of the medium surrounding the grating.

OPTIMIZING THE MICROSCOPE IMAGE: A COMPROMISE BETWEEN SPATIAL RESOLUTION AND CONTRAST

Putting these principles into practice, let us examine two specimens using transmitted light illumination and bright-field microscope optics: a totally opaque object such as a copper mesh electron microscope grid and a stained histological specimen. These objects are called *amplitude objects,* because light obscuring regions in the object appear as low-intensity, high-contrast regions when compared to the bright background in the object image. In comparison, transparent colorless objects such as living cells are nearly invisible, because the amplitude differences in the image are generally too small to reach the critical level of contrast required for visual detection. We discuss methods for visualizing this important class of transparent objects in Chapter 7.

With the microscope adjusted for Koehler illumination using white light, begin by opening the condenser front aperture to match the diameter of the back aperture of the objective lens to obtain maximum aperture angle and therefore maximal spatial resolution. This operation is performed using an eyepiece telescope or Bertrand lens while inspecting the back focal plane of the objective lens. Since this plane is conjugate with the condenser aperture, the edges of the condenser diaphragm appear when the diaphragm is sufficiently stopped down. With the telescope lens focused on its edges, open the diaphragm until its margins include the full aperture of the objective to obtain the maximum possible aperture angle. Expecting maximum resolution in normal viewing mode, we are surprised to see that the image of the opaque grid bars is gray and not

black, and that the overall contrast is reduced. Similarly, fine details in the histological specimen such as collagen bundles, cell organelles, and the edges of membranes and nuclei have low contrast and are difficult to distinguish. The overall impression is that the image looks milky and washed out — in short, unacceptable. The poor definition at this setting of the condenser diaphragm is due to polychromatic illumination, scattered light, and reduction in the degree of coherence of the contributing waves. However, considerable improvements in the quality of the image can be made by using a bandpass filter to restrict illumination to a limited range of wavelengths and by partially closing the condenser diaphragm.

Monochromatic light assures that chromatic aberration is eliminated and that unit diffraction spots in the image are all of uniform size. With white light, diffraction spot size varies by nearly a factor of 2, due to the presence of different color wavelengths, with the result that diffraction features in the image are somewhat blurred. Monochromatic illumination sharpens the image and increases contrast, particularly for objects with inherently low contrast. For color objects such as histological specimens that are to be examined visually or recorded with a gray-scale camera or black-and-white film, contrast can be improved dramatically by selecting filters with complementary colors: a green filter for pink eosin dye or a yellow filter for blue hematoxylin stain. A green filter, for example, removes all of the pink eosin signal, reducing the amplitude of eosin-stained structures and making them look dark against a bright background in a gray-scale image.

To our surprise, closing down the condenser diaphragm also has a pronounced effect: It increases the contrast and greatly improves the visibility of the scene (Fig. 6-6). The grid bars now look black and certain features are more readily apparent. There are several reasons why this happens: (1) Part of the improvement comes from *reducing the amount of stray light* that becomes reflected and scattered at the periphery of the lens. (2) Reducing the aperture *increases the coherence of light*; by selecting a smaller portion of the light source used for illumination, the phase relationships among diffracted rays are more defined, and interference in the image plane results in higher-amplitude differences, thus increasing contrast. (3) With reduced angular aperture, the unit diffraction spots comprising the image become larger, causing lines and edges to become thicker and cover a greater number of photoreceptor cells on the retina, thus making the demarcations appear darker and easier to see. Thus, the benefits of improved contrast and visibility might lead us to select a slightly stopped-down condenser aperture, even though spatial resolution has been compromised slightly in the process. If the condenser aperture is closed down too far, however, the image loses significant spatial resolution and the dark diffraction edges around objects become objectionable.

Thus, the principles of image formation must be understood if the microscope is to be used properly. A wide aperture allows maximal spatial resolution, but decreases contrast, while a smaller, constricted aperture improves visibility and contrast, but decreases spatial resolution. For all specimens, the ideal aperture location defines a balance between resolution and contrast. A useful guideline for beginners is to stop down the condenser aperture to about 70% of the maximum aperture diameter, but this is not a rigid rule. If we view specimens such as a diffraction grating, a diatom, or a section of striated muscle, stopping down the diaphragm to improve contrast might suddenly obliterate periodic specimen details, because the angular aperture is too small to allow diffracted light to be collected and focused in the image plane. In such a situation, the aperture should be reopened to whatever position gives adequate resolution of specimen detail and acceptable overall image visibility and contrast.

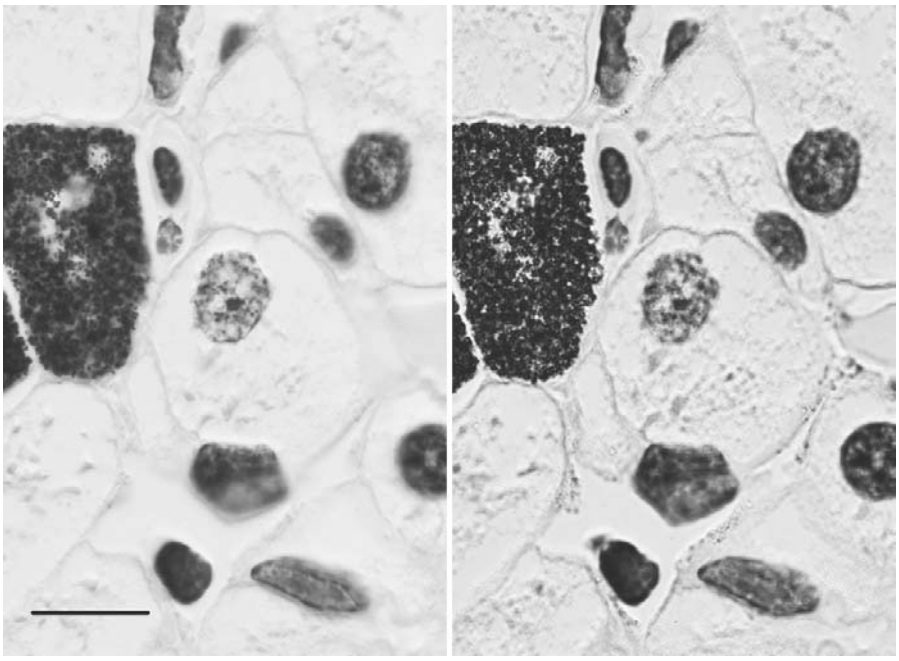

(a) (b)

Figure 6-6
Effect of the condenser aperture on image contrast and resolution. (a) With unrestricted aperture, resolution is maximal, but contrast suffers from stray light. (b) With the condenser aperture stopped down, light fills ~70% of the diameter of the back aperture of the objective. Contrast is improved, but resolution is reduced. Bright-field light micrograph of a hematoxylin-stained section of *Amphiuma* liver containing hepatocytes and pigment cells. Bar = 10 μm.

Exercise: Resolution of Striae in Diatoms

In this exercise we will use a diatom test plate to examine the effect of numerical aperture and wavelength on resolution in the light microscope. Diatoms are unicellular algae that produce shells of silica containing arrays of closely spaced pores. They have been used to determine the spatial resolution of objective lenses in microscopes for well over a century.

Diatoms belong to the class Chrysophyta of yellow-green and golden-brown algae. Their transparent quartz cell walls (valves or frustrules) are usually composed of two overlapping halves (valves) that contain semicrystalline and amorphous silica, which gives them a hard, brittle texture. The two overlapping valves are ornamented with tiny dots or perforations (pores) that are organized into rows (striae), both of which are commonly used to calibrate the magnification of microscopes. The ridge and pore spacings are constant for a given species. Figure 6-7 shows a diatom test plate obtained from Carolina Biological Supply Company,

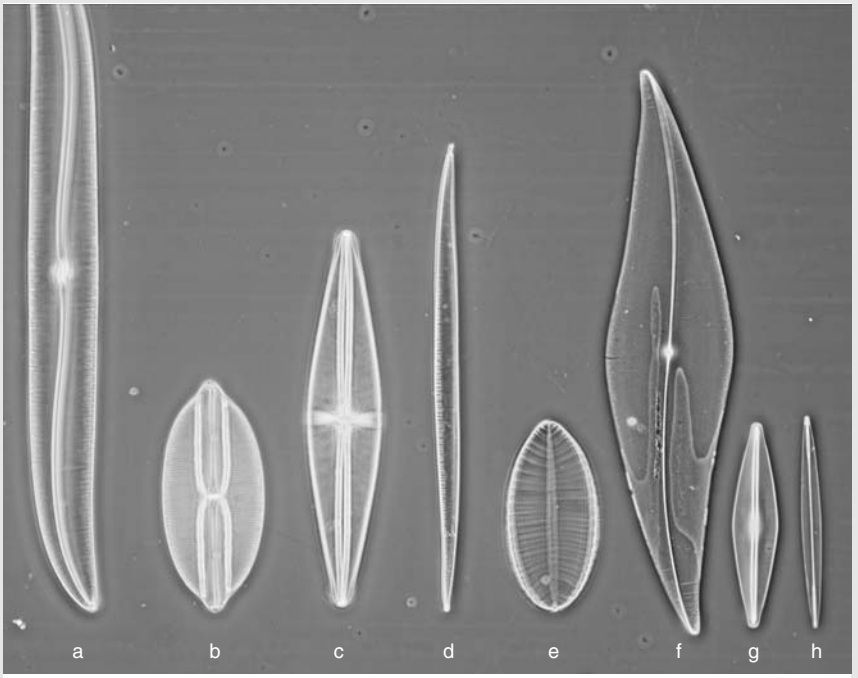

	Specimen	Length (μm)	Period (μm/stria)
a	*Gyrosigma balticum*	280	0.67
b	*Navicula lyra*	160	1.25
c	*Stauroneis phenocenteron*	150	0.71
d	*Nitzschia sigma*	200	0.43
e	*Surirella gemma*	100	0.50
f	*Pleurosigma angulatum*	150	0.53
g	*Frustulia rhomboides*	50	0.29
h	*Amphipleura pellucida*	80-140	0.27

Figure 6-7
Diatom test plate and key.

Burlington, North Carolina. The accompanying table indicates the cell size and interstria spacing for the eight species of diatoms on the plate. While performing this exercise, compare the image of *Pleurosigma* produced with a modern lens with that produced by one of the first apochromatic lenses designed by Abbe (Fig. 6-1). If a test plate is not available, use a grain of dispersed diatomaceous earth (from a chemical supply house), or, failing that, some household scrubbing cleaner, which contains diatom shells as an abrasive.

1. Review the steps for adjusting the microscope for Koehler illumination. Identify and locate the positions of the four aperture planes and the four

field planes, and prepare a list of each set in order, beginning with the lamp.

2. Adjust the condenser for bright-field mode. Image the diatom test plate using green light (546 nm bandpass filter) and a 40× objective. Focusing is difficult due to the extremely small size and transparent nature of the specimen. First locate the diatoms under low power (10×). Carefully move the x and y coordinates of the stage until the specimen comes into the field of view. Then swing in the 40× lens and refocus on the diatoms. Compare the image of the diatoms with Figure 6-7 and note the indicated spacings. Using bright-field optics and green light, open the condenser aperture to the proper location using the telescope lens, and note the species with the smallest spacing that it is possible to resolve with your microscope. Indicate the species and note the distance between the striae from the figure.
3. Calculate the theoretical resolution of the microscope under these conditions. The NA is indicated on the barrel of the lens. Show your work. The apparent and calculated resolution limits should roughly agree.
4. Now examine the diatom *Pleurosigma* with a dry 100× objective and close down the field-stop diaphragm to illuminate just this one diatom and no other. Make an accurate sketch of the hexagonal arrangement of the pores. Close down the condenser diaphragm to its minimum size. Now examine its diffraction pattern in the diffraction plane of the microscope using the telescope lens. Make an accurate sketch of the diffraction pattern.
5. How does the diffraction pattern relate to the spacing pattern of the diatom pores in the image plane?
6. Examine the diatoms in red and blue light and with the condenser aperture open or maximally closed. Which pair of conditions gives the lowest and the best resolution of the striae?
7. Examine the diatom *Pleurosigma* or *Diatoma* with a 100× oil immersion lens. Can the striae and pores be resolved? Examine the diffraction plane under these conditions. Make sketches of both views. Now oil the condenser as well as the objective and repeat your observations. Make sketches. Do you notice a difference in resolution?

CHAPTER

7

PHASE CONTRAST MICROSCOPY AND DARK-FIELD MICROSCOPY

OVERVIEW

Unstained objects such as cells present a unique problem for the light microscopist because their images generate very little contrast and are essentially invisible in ordinary bright-field microscopy. As we have seen, this is even true for transparent periodic specimens such as diffraction gratings and diatoms. Although transparent objects induce phase shifts to interacting beams of light due to scattering and diffraction, they remain nearly invisible, because the eye cannot detect differences in phase. In this chapter we examine two optical methods for viewing such objects: phase contrast microscopy, which transforms differences in the relative phase of object waves to amplitude differences in the image; and dark-field microscopy, where image formation is based solely on diffracted wave components. Phase contrast microscopy produces high-contrast images of transparent specimens such as cells and micro-organisms, tissue slices, lithographic patterns, and particles such as organelles. Living cells in tissue culture can also be examined directly, without fixation and staining (Fig. 7-1).

PHASE CONTRAST MICROSCOPY

In the case of stained, histological preparations or specimens with naturally occurring pigments, specific wavelengths are absorbed by dyes or pigments, allowing objects to appear in color when illuminated with white light. With monochromatic illumination using a color filter complementary to the color of the specimen for example, a blue object examined through a yellow filter object rays are significantly reduced in amplitude, resulting in a high-contrast image. Such objects are called *amplitude objects* because they directly produce amplitude differences in the image that are detected by the eye as differences in the intensity (Fig. 7-2). Although most transparent biological specimens do not absorb light, they do diffract light and cause a phase shift in the rays of light passing through them; thus, they are called *phase objects* (Fig. 7-2). The retardation imparted to a plane-wave front is shown in Figure 7-3. Phase contrast microscopes feature an optical design that transforms differences in the phase of object-diffracted waves to differences in the image, making objects appear as if they had been optically stained.

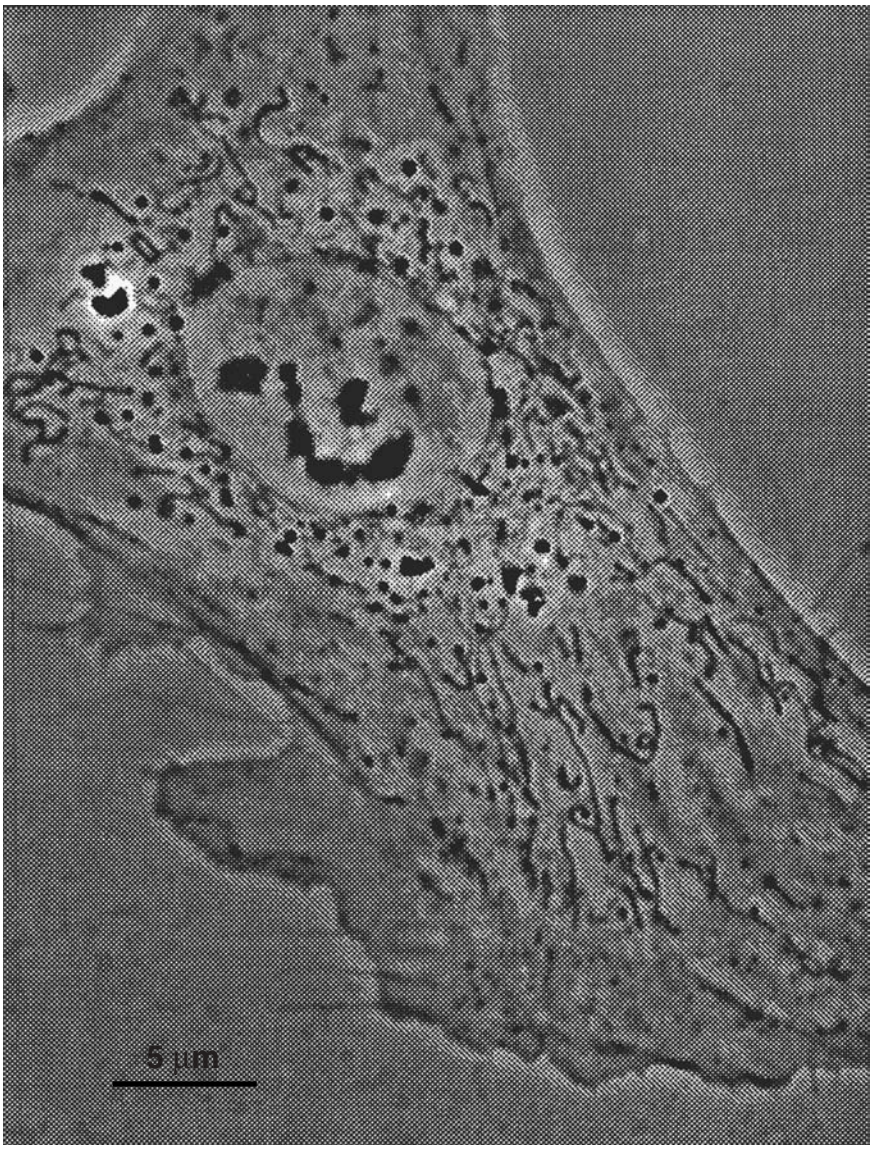

Figure 7-1

Phase contrast image of a living tissue culture cell. The cell nucleus, organelles, and membrane edges are clearly resolved in this normal rat kidney (NRK) cell. Phase-dense objects include mitochondria, lysosomes, and nucleoli, and domains of nuclear chromatin. Phase-light objects represent lipid droplets and small vesicles. Bar = 5 μm. (Specimen courtesy of Rodrigo Bustos, Johns Hopkins University.)

Because the method is dependent on diffraction and scattering, phase contrast optics also differentially enhance the visibility of the light scattering edges of extended objects and particles. The performance of modern phase contrast microscopes is remarkable. Under favorable conditions and with electronic enhancement and image processing, objects containing just a few protein molecules can be detected.

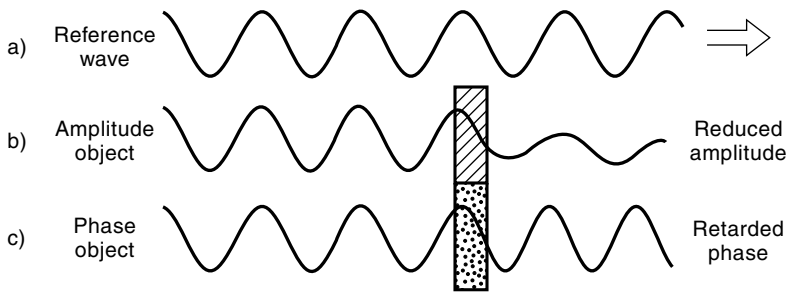

Figure 7-2

Effects of amplitude and phase objects on the waveform of light. (a) Reference ray with characteristic amplitude, wavelength, and phase. (b) A pure amplitude object absorbs energy and reduces the amplitude, but does not alter the phase, of an emergent ray. (c) A pure phase object alters velocity and shifts the phase, but not the amplitude, of an emergent ray.

In the 1930s, Frits Zernike, a Dutch physicist at the University of Groningen, created an optical design that could *transform differences in phase to differences in amplitude.* The development of phase contrast optics is a brilliant example of how basic research in theoretical optics led to a practical solution for viewing unstained transparent objects in the light microscope. The Zeiss optical works in Jena introduced phase contrast objectives and accessories in 1942, which transformed research in biology and medicine. For his invention and theory of image formation, Zernike won the Nobel prize in physics in 1953 (Fig. 7-4). Excellent descriptions of the technique are found in Bennett et al. (1951), Françon (1961), Slayter (1976), Slayter and Slayter (1992), and Pluta (1989).

In this chapter we first examine the process of image formation using the terminology and diagrams that are commonly employed to explain phase contrast optics. Then we examine the relative contributions of diffraction and differences in optical path length in generating the phase contrast image.

The Behavior of Waves from Phase Objects in Bright-Field Microscopy

WAVE TERMINOLOGY AND THE IMPORTANCE OF COHERENCE

Upon transit through a phase object, an incident wavefront of an illuminating beam becomes divided into two components: (1) an undeviated (0th-order) wave or *surround wave* (S wave) that passes through the specimen, but does not interact with it, and (2) a

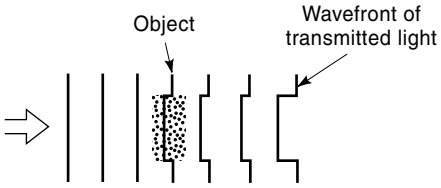

Figure 7-3

Disturbance by a phase object to an incident planar wavefront.

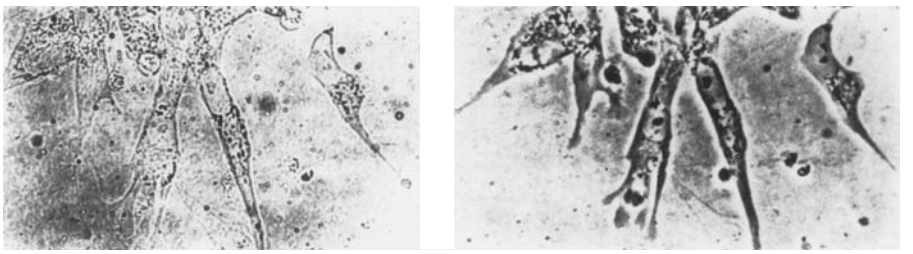

Figure 7-4

How I Discovered Phase Contrast. Modified excerpts from Dr. Zernike s Nobel prize address delivered in 1953 in Stockholm, Sweden, and published in the March 11, 1955, issue of *Science* (Zernike, 1955). Top: Dr. Zernike in his laboratory, November 1953. Bottom: Living tissue culture cells as seen with bright field (left) and phase contrast (right).

Phase contrast was not discovered while I was working with a microscope, but originated in my interest in diffraction gratings. About 1930 our laboratory obtained a large concave grating ruled by Robert Wood at Johns Hopkins University in Baltimore. Periodic errors in the grating lines made by ruling machines at that time caused the grating to exhibit a strongly striped surface, but when the grating was examined with a telescope at some 6 m distance and was exactly focused on the surface of the grating the stripes disappeared! By a succession of experiments and calculations I soon succeeded in explaining this. In a simpler case, a telescope was used to examine the phases of lines in a diffraction pattern of a vertical line-source of light after placing a 2 mm wide slit close behind the objective of the telescope. The diffraction maxima were observed but their phases could not be distinguished. However, the phases could be observed by throwing the diffraction image on a *coherent background* that served as a reference surface. Now I happened to know of a simple method Lord Rayleigh described in 1900 for making what I called *phase strips* glass plates with a straight groove 1 mm wide and etched with acid to a uniform depth of half a wavelength. When a phase plate was placed in the spectrum of the faulty grating and examined with the telescope, the strips on the grating surface now stood out clearly.

deviated or *diffracted wave* (D wave) that becomes scattered in many directions. Typically, only a minority of incident waves are diffracted by cellular objects. Both S and D waves are collected by the objective lens and focused in the image plane at the site corresponding to the image of the particle, where they undergo interference and generate a resultant *particle wave* (P wave). The relationship among waves is thus described as P = S + D. Detection of the object image depends on the intensities, and hence on the amplitudes, of the P and S waves. *Only when the amplitudes of the P and S waves are significantly different in the image plane can we see the object in the microscope.* Before beginning our explanation of the interference mechanism, we should note our earlier discussion of the coherence of light waves in the myriad small beams (wave bundles) illuminating the specimen (Chapter 5). This condition is of great practical importance for phase contrast microscopy, because image formation through constructive and destructive interference requires coherent illumination such that: (1) A definite phase relationship exists between the S and D waves, and (2) the phase relationship must be preserved between the object and the image.

DEPICTION OF WAVE INTERACTIONS WITH SINE WAVE AND VECTOR DIAGRAMS

With this general scheme in mind, let us now examine Figure 7-5a, which shows the S, D, and P waves as sine waves of a given wavelength in the region of the object in the image plane. The S and P waves, whose relative intensities determine the visual contrast, are shown as solid lines, whereas the D wave (never directly observed) is shown as a dashed line. The amplitude of each wave represents the sum of the E vectors of the component waves. The D wave is lower in amplitude than the S wave, because there are fewer D-wave photons than there are S-wave photons at the image point. Notice that the *D wave is retarded in phase by λ/4 relative to the S wave* due to its interaction with the object particle. The P wave resulting from interference between the D and S waves is retarded relative to the S wave by only a small amount ($\sim\lambda/20$) and has an amplitude similar to that of the S wave. *Since the S and P waves have close to the same amplitude*

For a physicist interested in optics it was not a great step to change over from this subject to the microscope. Remember that in Ernst Abbe s remarkable theory of the microscope image the transparent object under the microscope is compared with a grating. Abbe examined gratings made of alternating opaque and transparent strips (amplitude gratings). Gratings made of transparent alternating thick and thin strips (phase gratings) produce diffraction spots that show a phase difference of 90°. For a phase object, my phase strip in the focal plane of the microscope objective brought the direct image of the light source into phase with the diffracted images, making the whole comparable to the images caused by an amplitude object. Therefore the image in the eyepiece appears as that of an absorbing object that is, with black and white contrast, just as if the object has been stained.

On looking back on these events I am impressed by the great limitations of the human mind. How quick we are to learn that is, to imitate what others have done or thought before and how slow to understand that is, to see the deeper connections. Slowest of all, however, are we in inventing new connections or even in applying old ideas in a new field. In my case, the really new point was the diffraction pattern of lines of the grating artifacts, the fact that they differed in phase from the principal line, and that visualization of phases required projection of the diffraction image on a coherent background. The full name of the new method of microscopy might be something like phase-strip method for observing phase objects in good contrast. I shortened this to phase contrast.

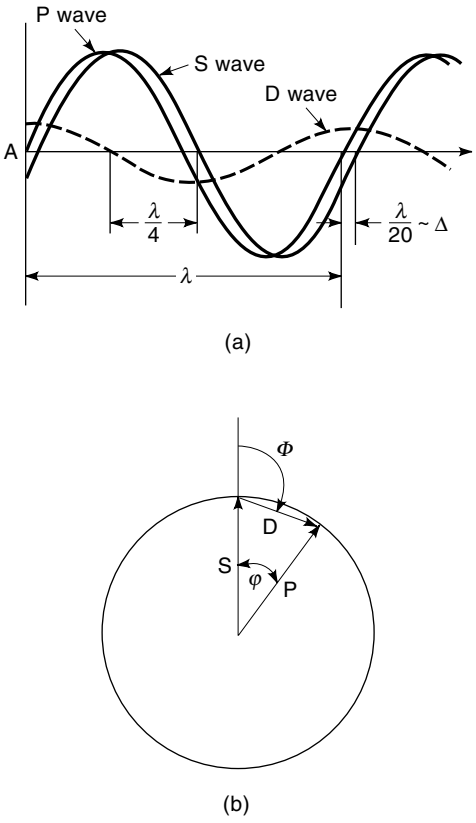

Figure 7-5

Phase relations between S, D, and P waves in bright-field microscopy. S and D waves, generated at the object, recombine through interference to generate the resultant particle image wave (P) in the image plane of the microscope (P = S + D). Relative to S, the D wave has a lower amplitude and is retarded in phase by ~λ/4. The slight phase shift of λ/20 in the resultant P wave is related to the optical path length difference and is typical for small object details in a cell. Since the amplitudes of the S and P waves are the same, the contrast is 0, and the object remains invisible against the background. (a) Wave components shown as sine waves. In this chapter, sine waves represent the amplitude and phase of a whole population of waves, not single photons. Thus, the lower amplitude of the D wave does not mean energy was absorbed, but rather that there are fewer D waves than there are S waves. (b) Vector diagram of S, P, and D waves. For explanation, see text.

in simple light microscopy, there is no contrast in the image and the object remains invisible.

The same situation can be described vectorially using a system of polar coordinates, where the length of a vector represents the amplitude of a wave, and the angle of rotation of the vector relative to a fixed reference (angular phase shift ϕ) represents the amount of phase displacement (Fig. 7-5b). Phase retardations are shown as clockwise rotations, whereas phase advancements are depicted as counterclockwise rotations. In this plot (technically a phasor diagram), the reconstructed P wave is shown as the vector sum of the S and D waves. This form of presentation is convenient because you can see more clearly how different degrees of phase shift in the D wave affect the phase of

the resultant P wave, and vice versa. A complete description of this form of wave analysis is given by Hecht (1998), Pluta (1989), and Slayter (1976), but for our purposes, a brief definition will be sufficient to explain the diagram. The phase shift of D relative to S on the graph is shown as Φ, where $\Phi = \pm 90° + \phi/2$, and ϕ is the relative phase shift (related to the optical path difference) between the S and P vectors. For objects with negligible optical path differences (phase shifts ϕ), Φ is $\pm 90°$. As shown in the figure, a D wave of low amplitude and small phase shift results in a P wave with an amplitude that is nearly equal to that of the S wave. With similar amplitudes for S and P, there is no contrast, and the object remains invisible.

The Role of Differences in Optical Path Lengths

We encountered the concept of optical path length previously when we discussed the action of a lens in preserving the constancy of optical path length between object and image for coherent waves emerging from an object and passing through different regions of the lens (Fig. 5-6). For phase contrast microscopy, we are concerned with the role of the object in altering the optical path length (relative phase shift ϕ) of waves passing through a phase object.

Since the velocity of light in a medium is $v = c/n$, where c is the speed of light in a vacuum, rays of light passing through a phase object with thickness t and refractive index n greater than the surrounding medium travel slower through the object and emerge from it retarded in phase relative to the background rays. The difference in the location of an emergent wavefront between object and background is called the *phase shift* δ (same as ϕ above), where δ in radians is

$$\delta = 2\pi\Delta/\lambda,$$

and Δ is the *optical path difference,* which was defined in Chapter 5 as

$$\Delta = (n_2 - n_1)t.$$

The Optical Design of the Phase Contrast Microscope

The key element of the optical design is to (1) isolate the surround and diffracted rays emerging from the specimen so that they occupy different locations in the diffraction plane at the back aperture of the objective lens, and (2) advance the phase and reduce the amplitude of the surround light, in order to maximize differences in amplitude between the object and background in the image plane. As we will see, the mechanism for generating relative phase retardation is a two-step process: D waves are retarded in phase by $\sim\lambda/4$ at the object, while S waves are advanced in phase by a phase plate positioned in or near the diffraction plane in the back aperture of the objective lens. Two special pieces of equipment are required: a condenser annulus and an objective lens bearing a phase plate for phase contrast optics.

The *condenser annulus,* an opaque black plate with a transparent annulus, is positioned in the front aperture of the condenser so that the specimen is illuminated by beams of light emanating from a ring (Fig. 7-6). (In some texts, the illuminating beam emergent from the condenser is described as a hollow cone of light with a dark center

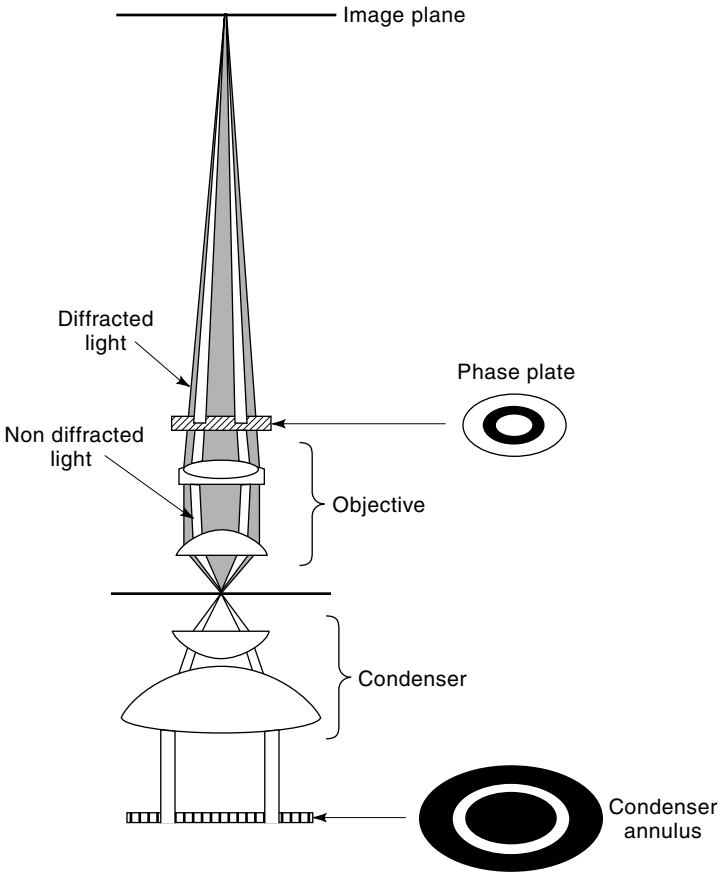

Figure 7-6

Path of nondiffracted and diffracted beams in a phase contrast microscope. An annular aperture in the front focal plane of the condenser generates a hollow cone of light that illuminates the specimen and continues (approximately) as an inverted cone that is intercepted by a phase plate at the back aperture of the objective lens. The image of the annulus is in sharp focus in this plane because it is conjugate to the front aperture plane of the condenser. Diffracted specimen rays fill the shaded region of the illumination path.

a concept that is useful but not strictly true.) The condenser annulus replaces the variable diaphragm in the front aperture of the condenser. Under conditions of Koehler illumination, S waves that do not interact with the specimen are focused as a bright ring in the back focal plane of the objective (the diffraction plane). Remember that under these conditions the objective s back focal plane is conjugate to the condenser s front aperture plane, so nondiffracted (0th-order) waves form a bright image of the condenser annulus at the back aperture of the objective. Light that is diffracted by the specimen (D waves) traverses the diffraction plane at various locations across the entire back aperture, the amount and location depending on the number, size, and refractive index differential of light-scattering objects in the specimen. Since the direct (0th-order light) and diffracted light become spatially separated in the diffraction plane, you can selectively manipulate the phase of either the S- or D-wave components.

To differentially alter the phase and amplitude of the direct (undeviated) light, a *phase plate* is mounted in or near the back focal plane of the objective (Figs. 7-6 and 7-7). In some phase contrast objectives, the phase plate is a plate of glass with an etched ring of reduced thickness to selectively advance the phase of the S wave by λ/4. The same ring is coated with a partially absorbing metal film to reduce the amplitude of the light by 70 75%. In other lenses the same effect is accomplished by acid etching a lens surface that is in or near the back focal plane of the objective lens. Regardless of the method, it is important to remember that phase contrast objectives are always modified in this way and thus are different from other microscope objectives.

The optical scheme for producing positive and negative phase contrast images is given in Figure 7-8. As discussed in the preceding section, the D wave emergent from the object plane is retarded by λ/4 relative to the phase of the S wave. In positive phase contrast optics (left side of the diagram), the S wave is advanced in phase by λ/4 at the phase plate, giving a net phase shift of λ/2, which now allows destructive interference with D waves in the image plane. Generally, the manipulation of relative phase advancement, while essential to phase contrast optics, is still unable to generate a high-contrast image, because the amplitude of the S wave is too high to allow sufficient contrast. For this reason, the ring in the phase plate is darkened with a semitransparent metallic coating to reduce the amplitude of the S wave by about 70%. Since P = S + D, interference in the image plane generates a P wave with an amplitude that is now considerably less than that of S. Thus, the difference in phase induced by the specimen is transformed into a difference in amplitude (intensity). Since the eye interprets differences in intensity as contrast ($C = \Delta I/I_b$), we now see the object in the microscope. (See Chapter 2 for discussion of formula.) *Positive phase contrast* systems like the one just described *differentially advance the phase of the S wave relative to that of the D wave.* Cellular objects having a higher refractive index than the surrounding medium are dark in appearance, whereas objects having a lower refractive index than the surrounding medium appear bright.

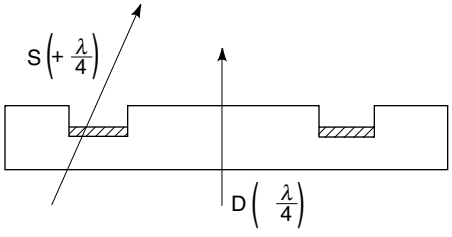

Figure 7-7

The action of a phase plate at the rear surface of the objective lens. Surround or background rays (S) are advanced in phase relative to the D wave by λ/4 at the phase plate. Relative phase advancement is created by etching a ring in the plate that reduces the physical path taken by the S waves through the high-refractive-index plate. Since diffracted object rays (D) are retarded by λ/4 at the specimen, the optical path difference between D and S waves upon emergence from the phase plate is λ/2, allowing destructive interference in the image plane. The recessed ring in the phase plate is made semitransparent so that the amplitude of the S wave is reduced by 70 75% to optimize contrast in the image plane.

It is also possible to produce optics giving *negative phase contrast,* where the S wave is retarded relative to the D wave, causing high-refractive-index objects to appear bright against a gray background. In this case, the phase plate contains an elevated ring that retards the phase of the 0th-order S wave relative to the phase of the D wave. The effect of this action in generating negative phase contrast is shown on the right-hand side of Figure 7-8.

Alignment

To form a phase contrast image, the rings of the annulus and phase plate must have matching diameters and be perfectly aligned. A multiple-position condenser with a rotating turret may contain two or three annuli intended for use with different phase contrast objectives. Small annuli are used for low-power dry objectives, whereas large annuli are employed with high-power, oil immersion lenses. The nomenclature used by different microscope companies varies, but the proper selection can always be made by matching the designation on the edge of the turret with the corresponding designation on the barrel of the objective lens. Whenever a lens is changed and a new annulus is brought into position, it is important to inspect the objective back aperture to make sure the annulus and the phase plate match and that they are aligned. Since the objective lens is usually fixed, alignment is performed by moving the condenser annulus with special annulus positioning screws on the condenser. The annulus adjustment screws, not to be confused with the condenser centration screws, are either permanently mounted on the condenser turret or come as separate tools that must be inserted into the condenser for this purpose. After bringing the rings into sharp focus with the telescope focus, move the bright image of the annulus to exactly coincide with the dark ring on the phase plate (Fig. 7-9). Improper alignment gives a bright, low-contrast image, because the bright background rays are not properly attenuated or advanced in phase as required by phase contrast theory.

Interpreting the Phase Contrast Image

Phase contrast images are easiest to interpret when the cells are thin and spread out on the substrate. When such specimens are examined in positive contrast mode, the conventional mode of viewing, objects with a higher refractive index than the surrounding medium appear dark. Most notably, phase contrast optics differentially enhance the contrast of the edges of extended objects such as cell margins. Generally, positive phase contrast optics give high-contrast images that we interpret as density maps. As an approximation, this interpretation is usually correct, because the amplitude and intensity in an object image are related to refractive index, and optical path length. Thus, a series of objects of increasing density (such as cytoplasm, nucleus, and nucleolus) are typically seen as progressively darker objects. However, the size and orientation of asymmetric objects also affect intensity and contrast. Further, there are optical artifacts we need to recognize that are present in every phase contrast image.

Interpreting phase contrast images requires care. In positive phase contrast optics, cell organelles having a lower refractive index than the surrounding cytoplasm generally appear bright against a gray background. Examples include pinocytotic vesicles, lipid droplets, and vacuoles in plant cells and protozoa. For objects that introduce relatively

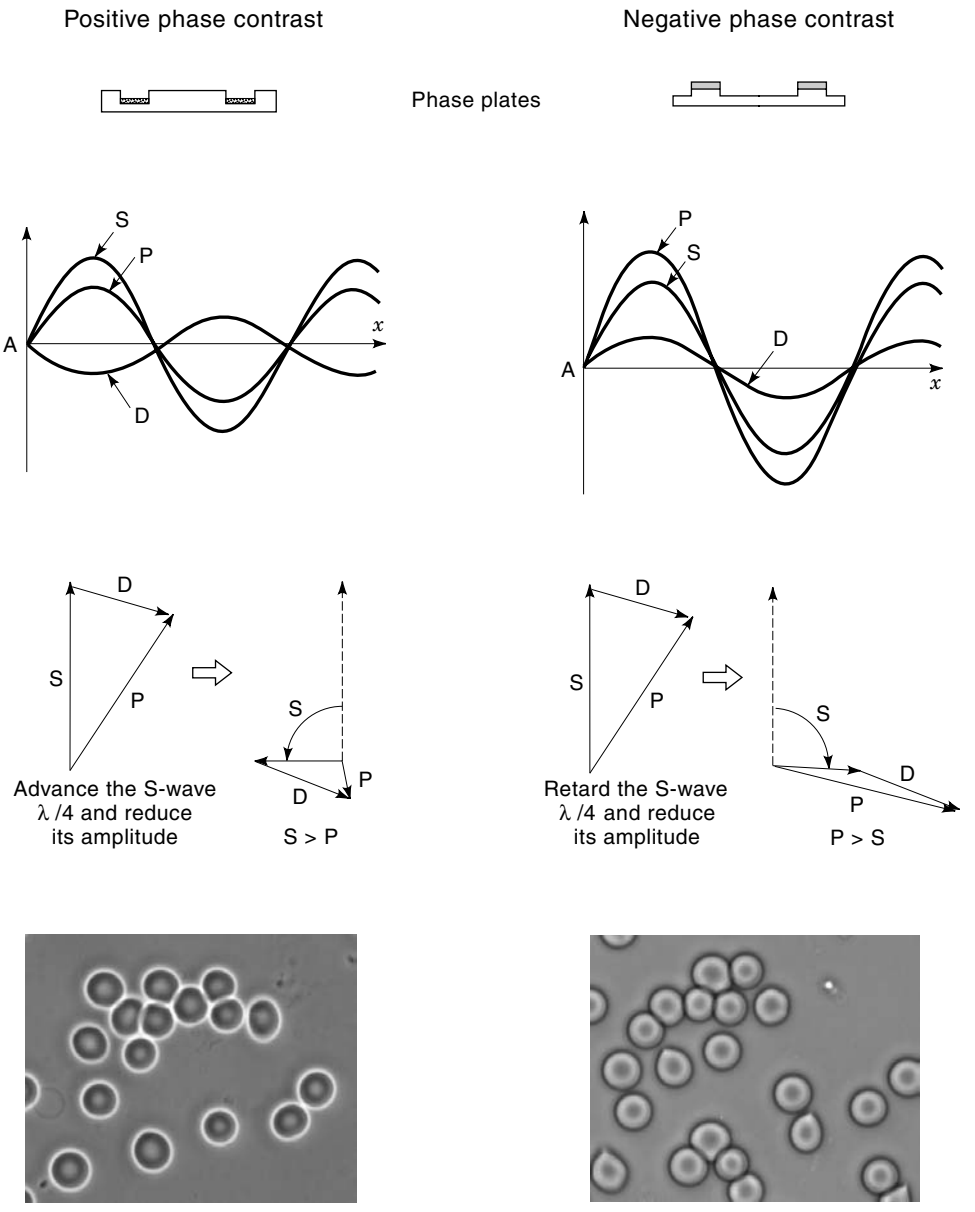

Figure 7-8

Comparison of positive and negative phase contrast systems. Shown in pairs, from the top down: phase plates for advancing (positive contrast) or retarding (negative contrast) the surround wave; amplitude profiles of waves showing destructive interference (positive phase contrast) and constructive interference (negative phase contrast) for a high-refractive-index object. Notice that the phase plate advances or retards the S wave relative to the D wave. The amplitude of the resultant P wave is lower or higher than the S wave, causing the object to look relatively darker or brighter than the background. Vector diagrams showing advancement of the S wave by $\lambda/4$, which is shown as a 90° counterclockwise rotation in positive phase contrast, and retardation of the S wave by $\lambda/4$, which is shown as a 90° clockwise rotation in negative phase contrast. Addition of the S and D wave vectors gives P waves whose amplitudes vary relative to the S waves. Images of erythrocytes in positive and negative phase contrast optics.

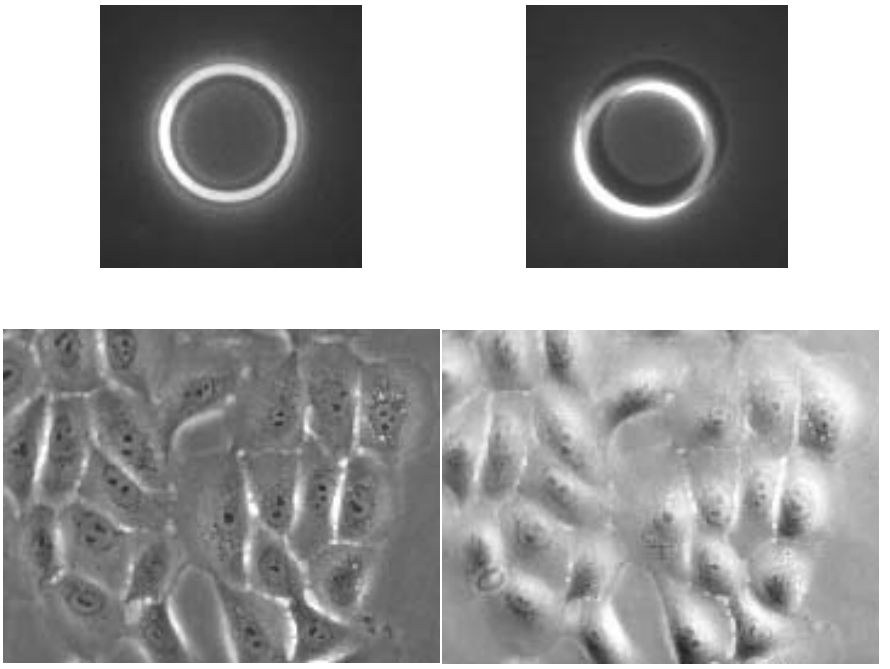

(a) (b)

Figure 7-9

Alignment of condenser and objective annuli. An eyepiece telescope or Bertrand lens is used to examine the back aperture of the objective lens. (a) The dark ring of the phase plate must be perfectly centered with the bright ring of light from the condenser annulus. The adjustment is made using two condenser plate-centering screws. These screws are distinct from the condenser centration screws, which are used to center the condenser lens with respect to the optic axis of the microscope. (b) Notice the low-contrast shaded image resulting from a misaligned annulus.

large phase retardations (phase shift Φ of the diffracted wave $\sim\lambda/2$), interference becomes constructive, making the objects appear brighter than the background.

To avoid confusion regarding bright and dark contrast in phase contrast images, it is useful to reconsider the term *optical path difference,* which is the product of refractive index and object thickness, and is related to the relative phase shift between object and background waves. It is common to hear microscopists refer to high- and low-refractive-index objects in a phase contrast image, but this is technically incorrect unless they know that the objects being compared have the same thickness. Thus, a small object with a high refractive index and a large object with a lower refractive index can show the same optical path difference and yet appear to the eye to have the same intensity (Fig. 7-10). In particular, conditions that cause shrinking or swelling of cells or organelles can result in major differences in contrast. Likewise, replacement of the external medium with one having a different refractive index can result in changes in image contrast.

Finally, phase contrast images show characteristic patterns of contrast halos and shade-off in which the observed intensity does not correspond directly to the optical path difference of the object. These patterns are sometimes referred to as phase artifacts or distortions, but should be recognized as a natural result of the optical system. *Phase halos* always surround phase objects and may be dark or light depending on whether the optical

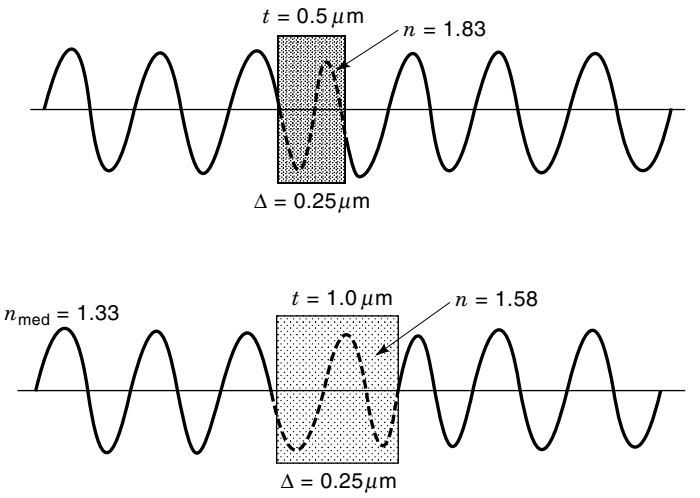

Figure 7-10

Effects of refractive index and specimen thickness on the optical path length. The phase contrast image reveals differences in optical path length as differences in light intensity, thus providing contrast. Since optical path length difference Δ is defined as the product of thickness t and refractive index n difference such that $\Delta = (n_1 - n_2)t$, two objects that vary both in size and refractive index can have the same optical path length and the same intensity in the phase contrast microscope.

path through an object is greater or less than that of the medium. (For examples, see Figures 7-1 and 7-8.) For objects that appear dark, the phase halo is light, and vice versa. Halos occur because the ring in the phase plate in the objective back aperture also receives some diffracted light from the specimen a problem accentuated by the fact that the width of the annulus generated by the 0th-order surround waves is smaller than the actual width of the annulus of the phase plate. Due to requirements of optical design, the difference in width is usually about 25%. Since diffracted rays corresponding to low spatial frequencies pass through the annulus on the plate, they remain 90° out of phase relative to the 0th-order light. The absence of destructive interference by these low-spatial-frequency diffracted waves causes a localized contrast reversal that is, a halo around the object. Halos are especially prominent around large, low-spatial-frequency objects such as nuclei and cells. Another contributing factor is the redistribution of light energy that occurs during interference in the image plane. As in the case of the diffraction grating and interference filter, interference results in a redistribution of light energy, from regions where it is destructive to regions where it is constructive. High contrast halos can be objectionable for objects generating large optical path differences such as erythrocytes, yeast cells, and bacteria. In many cases it is possible to reduce the amount of phase shift and diffraction and therefore the amount of halo, by increasing the refractive index of the medium using supplements such as glycerol, mannitol, dextran, or serum albumin. As will be seen in the next exercise, changing the refractive index of the medium can even reverse image contrast, turning phase-dark objects into phase-bright ones.

Shade-off is another optical effect that is particularly apparent in images of extended phase objects. In a phase contrast mechanism based solely on optical path differences (one that does not consider the effects of diffraction), you might expect that the

image of a large phase object of constant optical path length across its diameter would appear uniformly dark or light, but this is not the case. As shown schematically in Figure 7-11, the intensity profile of a phase-dark object gradually increases toward the center of the object. If the object is large enough, the light intensity in the central regions approaches that of the surrounding background. Shade-off is frequently observed on large, extended objects such as extended or flattened cells (Fig. 7-1), flattened nuclei, and planar slabs of materials, for example, mica or glass. The phenomenon is also known as the *zone-of-action effect,* because central uniform zones and refractile edge zones of an object diffract light differently. In central regions of an object, the amount of diffraction and the angle of scattering are greatly reduced. Object rays, although retarded in phase, deviate only slightly from the 0th-order component, and fall within the annulus of the phase plate. As a result, the amplitude and intensity of the central region are essentially the same as the background. The presence of shade-off in extended objects and the high image contrast at edges remind us that the phase contrast mechanism is principally one of diffraction and scattering.

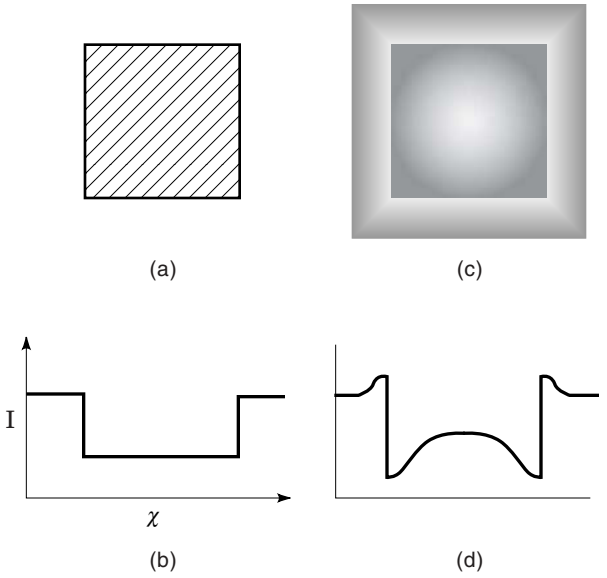

Figure 7-11
The effects of halo and shade-off in the phase contrast image. (a) Phase object. (b) Intensity profile of object shown in (a). (c) Phase object showing phase halo and shade-off. (d) Intensity profile of (c).

Exercise: Determination of the Intracellular Concentration of Hemoglobin in Erythrocytes by Phase Immersion Refractometry

In this exercise you will practice the proper alignment of phase contrast optics, examine blood cells in positive and negative contrast, and, using a series of solutions of varying refractive index, calculate the concentration of hemoglobin in your erythrocytes.

The phase shift of light, δ, which occurs when light passes through a cell with refractive index n_o in a medium with refractive index n_m, is given by $\delta = (n_o - n_m)\, t/\lambda$, where t is the thickness of the object and λ is the wavelength. The phase contrast microscope converts the phase shift into an observable change in amplitude. When $n_o > n_m$ (the case for most cellular structures), objects appear dark against a gray background (positive contrast). When $n_m > n_o$, objects look bright against a gray background (negative contrast). When $n_o = n_m$, no relative retardation occurs and the object is invisible. If blood cells are placed in a series of albumin solutions of increasing concentration (made isotonic by adjusting the concentration of NaCl to prevent shrinking and swelling due to osmotic effects), positive and negative cells can be counted under the phase contrast microscope and a curve can be constructed, and the isotonic point can be determined from the point at which 50% dark and bright cells are observed. This is a sensitive null method that can be used to obtain the concentration of solids in cells. In this case, we will calculate the intracellular molarity of hemoglobin in erythrocytes. *Note:* For erythrocytes, the intracellular concentration of hemoglobin is so high that cells look bright against a gray background when examined in normal isotonic saline. In the following exercise on erythrocytes, positive cells appear bright, and negative cells look dark.

1. Swab the tip of your finger with 70% ethanol and prick it with a sterile disposable lancet. Place a small drop of *fresh* blood (5 μL) on a microscope slide. Immediately place one drop (~60 μL) of albumin test solution on the droplet of blood, cover with a coverslip, and count the number of positive and negative cells 100 cells total for each sample. *Count only single cells that are seen face on. Do not count cell aggregates.* If necessary, you can check for invisible cells by turning away the condenser annulus, but perfect refractive index matching occurs only rarely, because the biconcave shape of the cells results in optical path differences through a single cell. Midpoint cells will appear both black and white simultaneously. It is recommended that you prepare and score one slide at a time. To recognize typical positive and negative cells, you should test the extreme albumin concentrations first. You should place your slides in a moist chamber (a sealed container with a moist paper towel) so that they do not dry out while you are busy counting other slides. Calculate the number of negative cells for each solution. Show your work.
2. Plot the % negative cells vs. mg/mL albumin on a piece of graph paper, and determine the concentration of albumin giving 50% positive and negative cells.
3. Given that hemoglobin has about the same specific refractive index increment as albumin and comprises 97% of the cell solids, having determined the concentration of albumin that is isotonic to the cells, calculate the molar concentration of hemoglobin in the erythrocytes. The molecular weight of native hemoglobin tetramer is 64,000 daltons. Treat the concentration (mg/mL) of bovine serum albumin (molecular weight, 67,000 daltons) as if it were hemoglobin, and use the molecular weight (of either) to calculate the molarity of hemoglobin in erythrocytes. How many times

more concentrated is hemoglobin in an erythrocyte than tubulin (2 μM) or aldolase (20 nM) in a fibroblast?

4. To what do you attribute the range of phase densities observed in the same erythrocyte sample? What are the estimated extremes of molarity of hemoglobin in your cells? How would you test if this is an artifact or represents real variation?

DARK-FIELD MICROSCOPY

In most forms of transmitted light microscopy, both the diffracted rays (rays that interact with the specimen) and nondiffracted rays (rays that pass undeviated through the specimen) are collected by the objective lens and contribute to image formation. For unstained transparent specimens, we have seen that the component of nondiffracted background light is very large, resulting in bright, low-contrast images in which details are poorly visible. Another solution for viewing such objects is *dark-field microscopy,* in which the nondiffracted rays are removed altogether so that the image is composed solely of diffracted wave components. This technique is very sensitive because images based on small amounts of diffracted light from minute phase objects are seen clearly against a black or very dark background. Dark-field microscopy is most commonly used for minute light-diffracting specimens such as diatoms, bacteria and bacterial flagella, isolated organelles and polymers such as cilia, flagella, microtubules, and actin filaments, and silver grains and gold particles in histochemically labeled cells and tissues. An example of a dark-field image of labeled neurons is shown in Figure 7-12. The number of scattering objects in the specimen is an important factor, because the scattering of light from too many objects may brighten the background and obscure fine details.

Theory and Optics

Dark-field conditions are obtained by illuminating the specimen at an oblique angle such that direct, nondiffracted rays are not collected by the objective lens. The effect of dark-field optics can be obtained quickly with bright-field optics by rotating the condenser turret so that rays illuminate the specimen obliquely. Only diffracted light from the specimen is captured by the objective, and the direct waves pass uncollected off to one side of the lens. The disadvantage of this technique is that unidirectional illumination of highly refractile objects can introduce large amounts of flare. Much better images are obtained with a special dark-field condenser annulus, which is mounted in the condenser turret. Special oil immersion dark-field condensers must be used for oil immersion objectives. Dark-field microscopy resembles phase contrast microscopy in that the specimen is illuminated by rays originating at a transparent annulus in the condenser. However, in dark-field optics only diffracted rays are collected by the objective and contribute to the image; nondiffracted rays are pitched too steeply and do not enter the lens (Fig. 7-13). Since nondiffracted background light is absent from the image, light-diffracting objects look bright against a dark field.

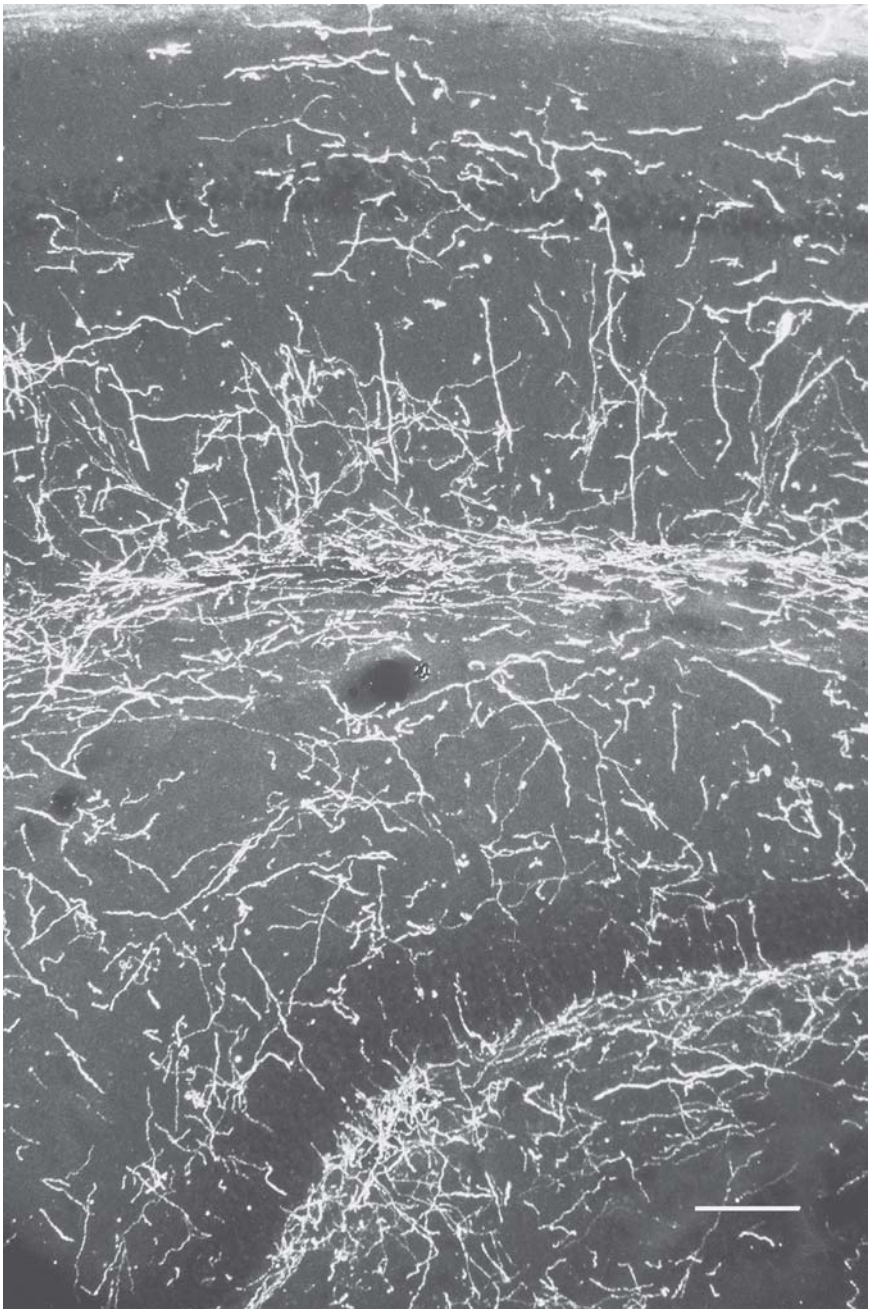

Figure 7-12

Dark-field image of neurons in a section of rat brain. Neurons were labeled with an axon-specific antibody conjugated to horseradish peroxidase. The section was developed with diaminobenzidine. The brown reaction product on the axons appears bright white in this dark-field light micrograph, which only reveals diffracted light components. Bar = 100 μm. (Image courtesy of Mark Molliver, Johns Hopkins University.)

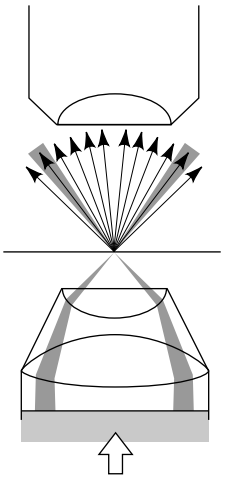

Figure 7-13

Optical scheme for dark-field microscopy. The geometry allows only diffracted light to be collected by the objective lens. Direct, nondiffracted rays are inclined at a steep angle and miss the objective entirely.

There are several ways to create a dark-field image:

Use the dark-field condenser stop, frequently labeled D on the condenser aperture turret, in combination with a medium power lens with NA < 0.8. If the NA of the objective is lower than the NA of the illuminating beam generated by the condenser and dark-field annulus, nondiffracted waves are excluded from the objective. If the objective lens contains an adjustable diaphragm, this can be stopped down slightly to help block any scattered direct rays that enter the lens.

An effective and economical approach is to use a phase contrast annulus that is intentionally oversized so that nondiffracted illuminating rays do not enter the objective lens that is, a high NA condenser annulus with a low NA objective.

For high magnification work requiring oil immersion objectives, you can employ special oil immersion dark-field condensers with parabolic or cardioid reflective surfaces (Fig. 7-14). These condensers reflect beams onto the specimen at a steeply pitched angle, giving a condenser NA of 1.2 1.4. A *paraboloid condenser* receives a planar wavefront and reflects it off a polished paraboloidal surface at the periphery of the condenser to a point in the specimen plane. The front aperture of the condenser contains an opaque glass with transparent annulus similar to that used in phase contrast microscopy. A *cardioid condenser* receives a collimated beam that is reflected at two surfaces to generate a steeply pitched beam for specimen illumination: A central convex spherical mirror reflects rays to a peripheral concave cardioidal mirror that defines the shape of the beam. Illumination by this condenser is aplanatic and thus free of both spherical aberration and coma. Since both condensers work by reflection, there is no chromatic aberration. The oil immersion objective lens used with these condensers should contain a built-in iris

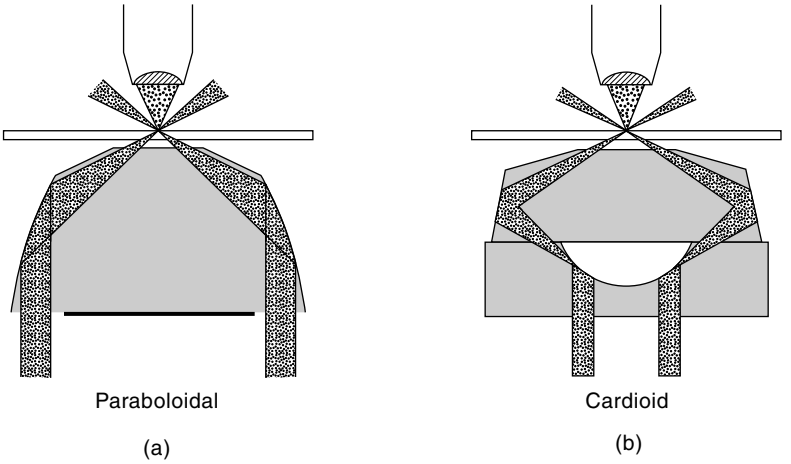

Figure 7-14

Two oil immersion dark-field condensers. (a) A paraboloid condenser receives a planar wavefront that is reflected off a polished paraboloidal surface to a spot in the specimen plane. The front aperture of the condenser contains an opaque glass with transparent annulus similar to that used in phase contrast microscopy. (b) A cardioid condenser receives a hollow cylinder of light, which is reflected by two spherical surfaces to generate a steeply pitched cone of light for specimen illumination: A central convex mirror reflects rays to a peripheral circumferential mirror with the figure of a cardioid, which reflects a steeply pitched cone of light onto the object.

diaphragm so that the numerical aperture can be reduced to 0.9 1.0 to exclude direct rays.

Image Interpretation

The appearance of a dark-field image is similar to one of self-luminous or fluorescent objects on a dark background, but with the difference that edges of extended, highly refractile objects diffract the greatest amount of light and dominate the image, sometimes obscuring the visibility of fainter, smaller objects. In addition, details in dark-field images are broader and less distinct compared to other imaging modes such as phase contrast, because removal of one entire order of light information from the diffraction plane makes edge definition less distinct in the image. Further, if the NA of the objective selected is too restricted, many diffracted waves are also eliminated, resulting in a loss of definition of fine details in the specimen.

In summary, dark-field optics are advantageous because they allow detection of weak diffracted light signals, and may be the method of choice for viewing fine structural details. Specimens as small as lysosomes, bacterial flagella, diatom striae, and microtubules are all easily seen in well-adjusted dark-field optics, even though these structures have dimensions that are ~20-times less than the resolution limit of the light microscope. Dark-field optics are also inexpensive, simple to employ, and generally do not require special equipment such as DIC prisms, strain-free lenses, or phase contrast objectives.

Exercise: Dark-Field Microscopy

1. Adjust the microscope for dark-field mode using a low-NA objective (10× or 20×) and a high-NA phase contrast or dark-field annulus. These annuli produce steeply pitched cones of light that are not accepted by low-NA, 10× or 20× objectives. Only the scattered light is accepted, which is what you want.
2. With the microscope adjusted for Koehler illumination, focus on a few isolated buccal epithelial cells (obtained by scraping of the underside surface of the tongue) and compare with the image obtained by phase contrast microscopy. Notice that object edges are enhanced by both of these modes of microscopy. In dark-field, each speck of dirt is imaged as a beautiful Airy disk surrounded by higher-order diffraction rings. This is an excellent chance to see the Airy disk, the diffraction pattern of a point source of light.
3. Using an oil immersion dark-field condenser (NA 1.4) and a 60× or 100× oil immersion objective, focus on the cilia and flagella of unicellular protozoa and algae. Cultures of protozoa can be obtained commercially, but a drop of pond water will do as well. *Note:* If the objective lens contains an aperture diaphragm, try stopping it down to improve contrast and visibility, as minute structures are difficult to detect.

The following specimens are suggested for dark-field examination:

Buccal epithelial cells

Culture of protozoa

Axons and glial cells in sections of rat brain labeled with antibodies adsorbed on gold colloid particles

Blood cells in a 60 μL drop of phosphate-buffered saline

Taxol-stabilized microtubules in 15 mM imidazole, 1 mM Mg-GTP, 5 μM taxol. The microtubule stock is ~5 10 mg/mL. Dilute to 0.1 mg/mL for observation. Difficult specimen!

Flagella of *Escherichia coli* bacteria. Difficult specimen!

CHAPTER

8

PROPERTIES OF POLARIZED LIGHT

OVERVIEW

In this chapter we turn our attention to polarization microscopy and a unique class of molecularly ordered objects that become visible upon illumination with polarized light. Figure 8-1 demonstrates the unique ability of a polarizing microscope to reveal molecular order in crystals and starch grains found in plant cell cytoplasm. Polarized light is also used in interference microscopy, including differential interference contrast (DIC) microscopy. Although we can observe high-contrast images of ordered objects using a polarizing microscope, it is remarkable that the eye has no ability in the usual sense to distinguish polarized light from random light. For this we require special filters called polarizers, retarders, and compensators. The relationships between the physics of polarized light and images of molecularly ordered specimens are remarkable in their economy and precision and are well worth mastering. Since the topic of polarized light is technically demanding, we use this chapter to describe its generation, properties, and interaction with different objects and optical devices. Our goal is to understand the working principles of the polarizing microscope, which is described in Chapter 9. Our reward will be in appreciating how the polarizing microscope reveals patterns of molecular order that otherwise can only be studied using more expensive, technically difficult methods such as electron microscopy or X-ray diffraction that operate at the resolution limit of molecules and atoms.

THE GENERATION OF POLARIZED LIGHT

The bulk light from most illuminators used in light microscopy is nonpolarized, the E vectors of different rays vibrating at all possible angles with respect to the axis of propagation (Fig. 8-2a). In a ray or beam of *linearly polarized light,* the E vectors of all waves vibrate in the same plane; the E vectors of beams of polarized light covering an extended area are *plane parallel.* Since the plane of vibration of the E vector can occur at any angle, to describe the orientation of the plane in a beam cross section we describe the angle of tilt relative to a fixed reference plane designated 0° (Fig. 8-2b). A device

Figure 8-1

Crystals and starch grains in *Amaryllis* cytoplasm as seen in a polarizing microscope. The high contrast indicates a high degree of molecular order in these structures.

that produces polarized light is called a *polarizer;* when used to determine the plane of vibration, the same filter is called an *analyzer.* The most efficient polarizers are made of transparent crystals such as calcite, but polarized light can also be generated simply and economically using a partially light-absorbing sheet of linear polarizing material of the type originally introduced by the Polaroid Corporation. Linear polarizers have a unique transmission axis (usually marked on the plate) that defines the plane of vibration of the transmitted rays. Polarizers also play an important role as an analytic tool for determin-

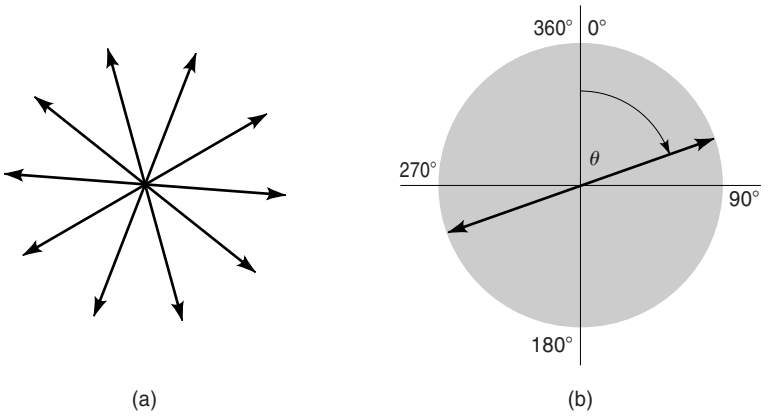

Figure 8-2

Random vs. linearly polarized light. The drawings show two beams of light, each containing several photons, as they would appear in cross section, looking down the axis of the beam. Refer to Figure 2-2 for orientation. (a) Random light: The E vectors of the waves are randomly oriented and vibrate in all possible planes. (b) Linearly polarized light: The E vectors of all waves comprising the beam vibrate in a single plane. The angle of the plane of vibration of the E vector relative to the vertical reference line is designated θ. The angle of tilt is called the azimuthal angle.

ing the orientation of polarized light whose plane of vibration is not known. Two linear polarizers a polarizer and an analyzer are incorporated in the optics of a polarizing microscope.

Demonstration: Producing Polarized Light with a Polaroid Filter

A *Polaroid sheet,* or *polar,* is a polarizing device that can be used to demonstrate linearly polarized light. The sheet has a transmission axis, such that incident waves whose E vectors vibrate in a plane parallel to the axis pass through the filter, while other rays are absorbed and blocked (Fig. 8-3). Because of its unique action, the Polaroid sheet can be used to produce linearly polarized light or to determine the plane of vibration of a polarized beam whose orientation is not known. Used in these ways, the sheet is then called, respectively, a polarizer or an analyzer. To become familiar with polarized light, perform the following operations using a pair of Polaroid sheets:

> Place two polars on top of each other on a light box and rotate one of the polars through 360°. At two azimuths separated by 180°, light transmission reaches a maximum, while at two azimuths separated from the first two by 90°, transmission is substantially blocked, and the field looks black. In the first case, light is transmitted because the transmission axes of the two polars are parallel, and all of the light transmitted by the first filter passes through

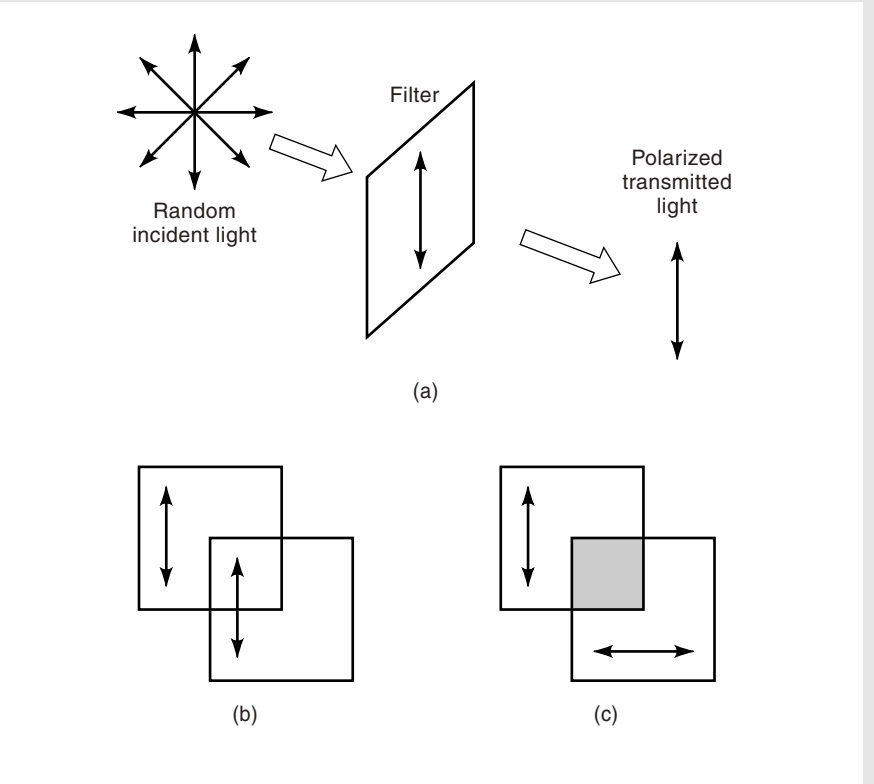

Figure 8-3
A Polaroid sheet generates linearly polarized light. (a) Only rays whose E vectors vibrate in a plane parallel with the transmission axis of the sheet are transmitted as a linearly polarized beam; other rays are partially transmitted or blocked. (b) A second overlapping polar transmits light of the first polar if its transmission axis is parallel to that of the first polar. (c) Transmission is completely blocked if the transmission axes of the two polars are crossed.

the second. The removal of light at the unique crossed position is called *extinction.* Here, polarized light from the first filter vibrates in a plane that is perpendicular to the transmission axis of the second filter and is substantially blocked by the second filter.

Examine a beam of light reflected off a flat nonconducting surface (glass or plastic) with a polar while rotating it through 360°. The reflected beam is minimized at two azimuths, indicating that it is partially linearly polarized. Used this way, the Polaroid sheet is called an analyzer. If the transmission axis of the polar is known beforehand, you should be able to observe that the plane of vibration of the reflected rays is parallel to the plane of the reflecting surface. If the transmission axis of a polar is not known, inspection of a reflected beam can be used to determine the approximate orientation of its transmission axis.

Using two crossed polars positioned on a light box, examine a piece of glass such as a microscope slide and a sheet of cellophane, while rotating them between the polars. The glass does not interact with polarized light and remains essentially invisible. Such materials are said to be *optically isotropic.* However, rotation of the cellophane sheet through 360° reveals four azimuths separated by 90° at which the entire sheet looks very bright. The unique ability of cellophane to interact with polarized light is due to the presence of aligned parallel arrays of cellulose molecules and birefringence, which is described later in the chapter. Materials of this type are said to be *optically anisotropic.* All objects suitable for polarization microscopy exhibit some degree of molecular orientation and optical anisotropy.

POLARIZATION BY REFLECTION AND SCATTERING

Polarized light is also produced by a variety of physical processes that deflect light, including refraction, reflection, and scattering. Light reflected from the surfaces of dielectric materials is partially linearly polarized, with the E vectors of the reflected waves vibrating parallel to the reflecting surface and the extent of polarization increasing with decreasing angles of incidence. For light incident on a transparent material such as water or glass, there is a unique angle known as *Brewster s angle,* at which the reflected waves are completely plane polarized (Fig. 8-4). For the simple case of a beam of incident light travelling through air ($n = 1$), the critical angle is given as

$$\tan\theta = n.$$

For water ($n = 1.33$) and glass ($n = 1.515$) the critical angles are 53° and 57°, respectively. As an interesting note on reflection polarization, manufacturers of Polaroid sunglasses mount sheets of polarizing material in the frames with the transmission axis of the Polaroids oriented perpendicularly in the field of view. Bright reflections off horizontal surfaces, such as the roofs of cars or water on a lake, are very efficiently blocked, while the random light is partially blocked, since only vertically polarized rays can reach the eye.

Linearly polarized light is also produced by light scattering. A common example is the polarization of light in the northern sky caused by the scattering of sunlight by air molecules. The extent of polarization (~50%) is readily appreciated on a clear day by rotating a polarizer held close to the eye. In accordance with principles of scattering, polarization is maximal at an angle 90° from the sun. For additional information on polarization by refraction, reflection, and scattering, see the interesting discussions by Minnaert (1954) and Hecht (1998).

VECTORIAL ANALYSIS OF POLARIZED LIGHT USING A DICHROIC FILTER

The Polaroid sheet just described commonly consists of a film of parallel arrays of linear polyvinyl alcohol molecules with embedded polyiodide microcrystals (H-ink)

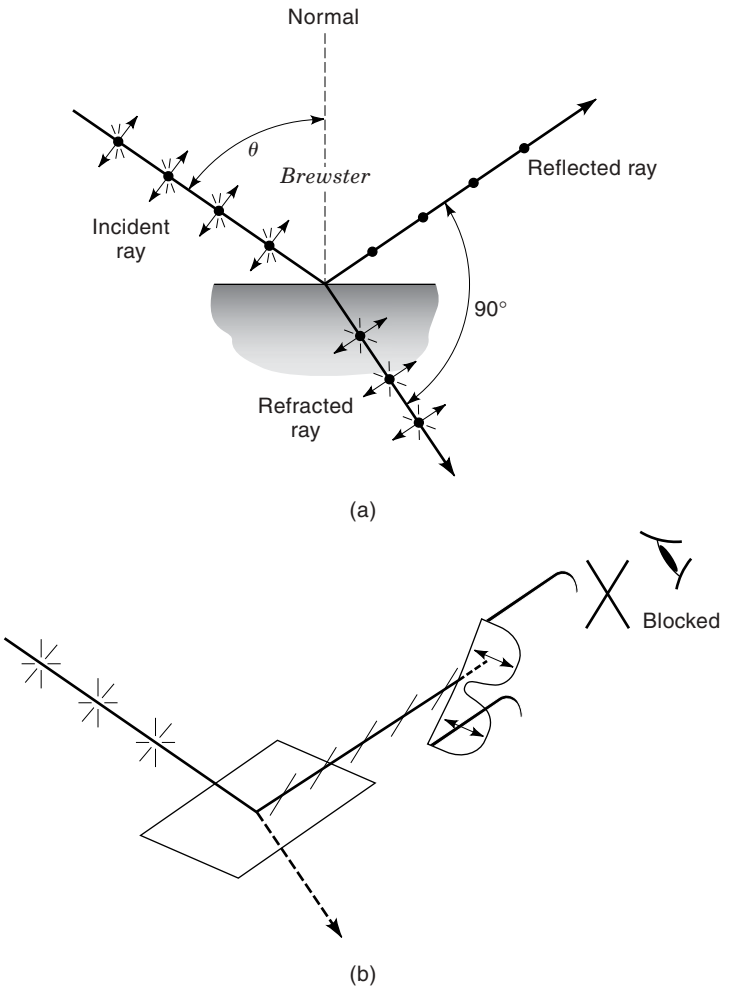

Figure 8-4

Reflection polarization and Brewster s critical angle. (a) The drawing shows an incident ray of random light (E vectors at random orientations) being reflected off a horizontal surface (glass or other dielectric material) as a linearly polarized beam to the eye. At a certain critical angle (Brewster s angle θ), the degree of polarization of the reflected ray is 100% and the E vectors of reflected rays vibrate in a plane that is perpendicular to the plane of incidence (the plane defined by the incident, reflected and refracted rays). The refracted ray, oriented at a 90° angle with respect to the reflected ray, is only partially polarized. (*Note:* Brewster s angle is defined by the condition that exists when the reflected wave is at 90° to the refracted wave; the phenomenon occurs because in the second medium the electric vector of the component in the plane of incidence is pointing in the direction of propagation of the reflected wave and consequently has no resultant wave in that direction.) (b) A Polaroid sheet can be used to demonstrate the polarized nature of the reflected ray. If the transmission axis of the Polaroid is oriented at 90° with respect to the vibrational plane of the reflected ray, transmission is blocked. This principle is used to advantage in the design of Polaroid sunglasses to reduce or eliminate reflective glare.

aligned in the same direction as the organic matrix. The transmission axis of the filter is perpendicular to the orientation of the crystals and linear polymers in the filter. Thus, rays whose E vectors vibrate parallel to the crystal axis are absorbed. Waves with oblique orientations are partially absorbed, depending on the azimuths of their vibrational planes. Filters such as the Polaroid sheet that differentially transmit rays vibrating in one plane while absorbing those in other planes are said to exhibit *dichroism;* hence the common name, *dichroic filter.* As we will see in later sections, the Polaroid sheet is a special kind of beam splitter designed to transmit rays vibrating at a certain azimuthal angle as linearly polarized light. For H-series filters that are commonly employed in microscopy, only about 25% of incident random light is transmitted, but the degree of polarization of the transmitted rays is $> 99\%$.

If two polarizers are oriented so that their transmission axes are perpendicular to each other, they are said to be crossed, and all of the light transmitted by the polarizer (now linearly polarized) is extinguished by the analyzer (Fig. 8-3). The extent to which incident random light is extinguished by two crossed polars is called the *extinction factor* and is defined as the ratio of the intensity of transmitted light observed for two polars when positioned in parallel and in crossed orientations ($I_{\parallel}/I_{\times}$). Extinction factors of 10^3 10^5 or greater are required for polarization microscopy and can be obtained using two dichroic filters.

The role of the analyzer in controlling the transmission of polarized light can be understood from vector diagrams showing the angular orientation (azimuthal angle) and magnitude of the E vectors of rays drawn from the perspective of viewing a ray end on, down its axis of propagation. Figure 8-5 shows a vertically oriented analyzer, four incident waves of linearly polarized light that are equal in amplitude but vibrating in different planes, and the amplitudes of those waves after transmission through the analyzer. If each incident wave is resolved into its horizontal and vertical components, it can be seen that the entire vertical component of each ray passes through the analyzer. Further, the amplitudes of the vertical component and the transmitted ray rapidly decrease as the plane of vibration of the incident ray approaches an azimuth perpendicular to the transmission axis of the analyzer.

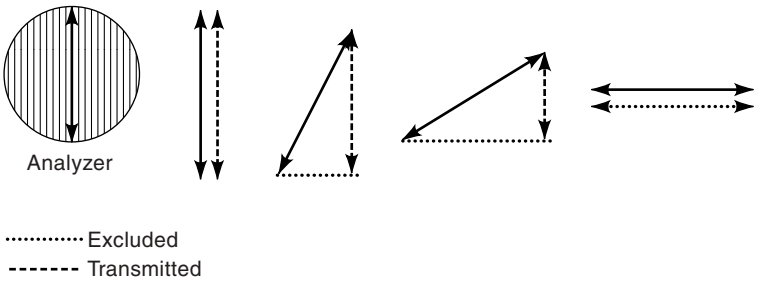

Figure 8-5

Transmission through an analyzer of linearly polarized rays vibrating in different planes. A linearly polarized ray vibrating at an azimuthal angle different from the transmission axis of an analyzer can be resolved into its horizontal and vertical components using principles of vector math. The amplitude of the transmitted ray is equal to the vertical vector component.

The amount of light transmitted through two polars crossed at various angles can be calculated using *Malus law,* which states that

$$I = I_o \cos^2\theta,$$

where I is the intensity of light passed by an analyzer, I_o is the intensity of an incident beam of linearly polarized light, and θ is the angle between the azimuth of polarization of the incident light and the transmission axis of the analyzer. Thus, for two polars crossed at a 90° angle, $\cos^2\theta = 0$, and $I = 0$, so polarized light produced by the first filter (the polarizer) is completely excluded by the second filter (the analyzer). For polarizers partially crossed at 10° and 45°, the light transmitted by the analyzer is reduced by 97% and 50%, respectively.

DOUBLE REFRACTION IN CRYSTALS

Many transparent crystals and minerals such as quartz, calcite, rutile, tourmaline, and others are optically anisotropic and exhibit a property known as *double refraction.* When letters on a printed page are viewed through a calcite crystal, remarkably each letter appears double (Figure 8-6). Calcite is therefore said to be *doubly refracting,* or *birefringent.* Birefringent materials split an incident ray into two components that traverse different paths through the crystal and emerge as two separate rays. This occurs because atoms in crystals are ordered in a precise geometric arrangement causing direction-dependent differences in the refractive index. In contrast, a sheet of glass, such as a microscope slide, which is an amorphous mixture of silicates, is usually optically isotropic and does not exhibit double refraction.

When a ray of light is incident on a birefringent crystal, it usually becomes split into two rays that follow separate paths. One ray, the *ordinary ray* or *O ray,* observes the laws of normal refraction, while the other ray, the *extraordinary ray* or *E ray,* travels along a different path. Thus, for every ray entering the crystal there is a pair of O and E rays that

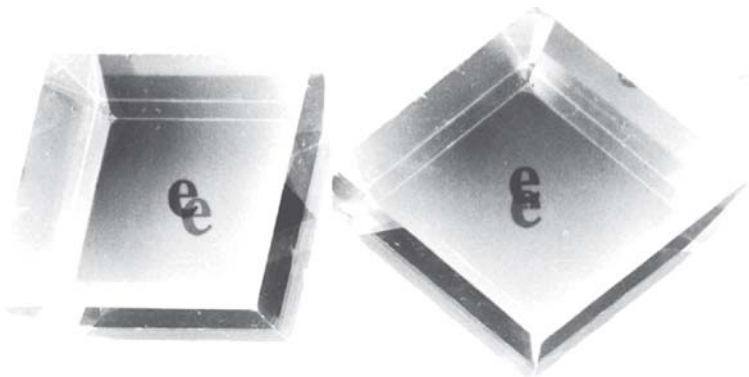

Figure 8-6

Double refraction in a calcite crystal. A letter viewed through a plane surface of the crystal appears double, the two images corresponding to the ordinary and extraordinary rays. As the crystal is rotated, the E ray rotates around the O ray. The O ray obeys the normal laws of refraction and does not rotate.

emerges, each of which is linearly polarized. *The electric field vectors of these two rays vibrate in mutually perpendicular planes.* A sketch depicting this phenomenon is shown in Figure 8-7a. These features are easily observed by placing a crystal of calcite on a printed page and looking down on the crystal while rotating a dichroic filter held in front of the eye (see Demonstration); the double letters become alternately visible and invisible as the filter is rotated through an angle of 90°. There are two unique angles of incidence on the crystal for which the behavior is different (1) The calcite crystal and others of its class contain a single unique axis known as the *optic axis.* Incident beams that are perpendicular to the optic axis are split into O and E rays, but the trajectories of these rays are coincident (Fig. 8-7b). At this unique angle of incidence, the O and E rays emerge at the same location on the crystal surface, but have different optical path lengths and are therefore shifted in phase. *This geometry pertains to most biological specimens that are examined in a polarizing microscope.* (2) Incident rays that follow trajectories parallel to this axis behave as ordinary rays and are not split into O and E rays (Fig. 8-7c). Under these conditions of illumination, calcite behaves as if it were optically isotropic, like glass. (It is difficult to demonstrate the optic axis of calcite because it runs obliquely across the diameter of the crystal, and it is necessary to look down crystal edges. One solution is to examine a specially prepared slab cut perpendicularly to the optic axis of the crystal.) These principles are displayed clearly in Hecht (1998), Pluta (1988), and Wood (1964).

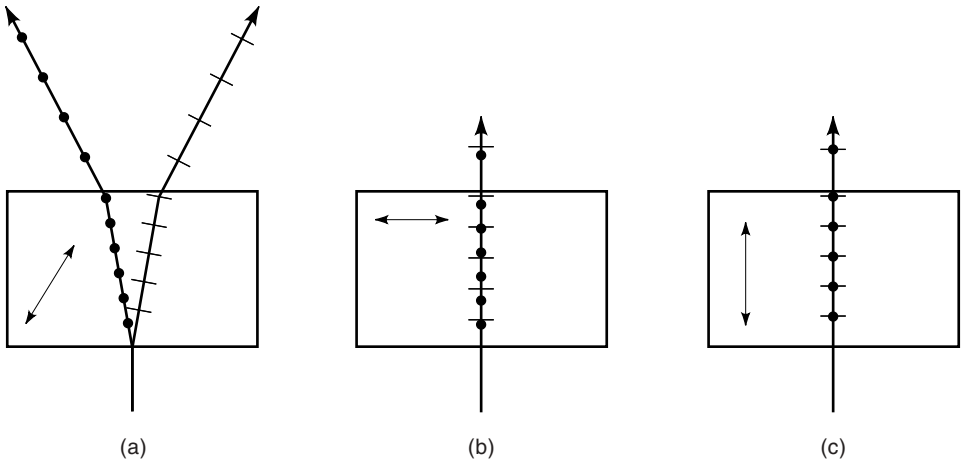

Figure 8-7

Splitting of an incident ray into O- and E-ray components by a birefringent crystal. The rectangular slabs shown in a, b, and c have been cut from parent crystals in such a way that the optic axes are oriented differently. Incident light is linearly polarized. Dots and dashes indicate the planes of vibration of linearly polarized O and E rays. Dots indicate the vibrations of E vectors that are perpendicular to the plane of the page, while the space between the dots represents one wavelength; dashes indicate vibrations parallel to the plane of the page. (a) A ray incident on a crystal at an angle oblique to the optic axis of the crystal is split into O and E rays that traverse different physical paths through the crystal. The emergent O and E rays are linearly polarized, vibrate in mutually perpendicular planes, and exhibit an optical path difference. (b) An incident ray whose propagation axis is perpendicular to the optic axis is split into O and E rays, but the two rays follow the same trajectory through the crystal and do not diverge. Emergent rays can exhibit an optical path difference. This is the usual case for birefringent biological specimens. (c) An incident ray whose propagation axis is parallel to the optic axis is not split and behaves as an ordinary ray. The optical path lengths of the emergent rays are the same.

Demonstration: Double Refraction by a Calcite Crystal

Place a crystal on a page of printed text and rotate the crystal while looking down on it from above. One ray does not move as the crystal is rotated (the O ray), whereas the other ray (the E ray) rotates around the fixed ray according to the angle of rotation of the crystal (Fig. 8-6). The O ray does not move because it obeys the laws of normal refraction and passes through the crystal on a straight, undeviated trajectory. The E ray, in contrast, travels along a tilted or oblique path, and its point of emergence at the surface of the crystal changes depending on the orientation of atoms in the crystal and therefore on the orientation of the crystal itself. Because the angle of divergence is so great, wedges of calcite crystal can be cut and glued together in such a way that one of the two components is reflected and removed while the other is transmitted, making calcite an ideal linear polarizer.

Examine the crystal resting on a black spot on a blank page through a dichroic polarizing filter held close to the eye, while rotating the crystal through 360°. First one ray and then the other ray alternately comes into view and becomes extinguished, and the black spot appears to jump back and forth as the filter is rotated through increments of 90°. The double images correspond to the O and E rays, each of which is linearly polarized and vibrates in a plane perpendicular to the other. For most crystals the two rays are close together and must be magnified to be observed, but in calcite the rays are so widely separated that no magnification is necessary. As we will see, this is due to large differences in the refractive index along different paths through the crystal. Notice too that polarized light cannot be distinguished from ordinary random light and that an analyzer is required to distinguish the different planes of polarization.

Materials such as calcite, quartz, and most molecularly ordered biological structures that contain a single optic axis are called *uniaxial.* Another class of *biaxial* crystals with two optic axes also exists, but is rarely encountered in biological systems. Biological examples of ordered macromolecular assemblies that can be seen in the polarizing microscope include such objects as lipid bilayers, bundles of microtubules and actin filaments, plant cell walls, crystalline granules of starch, lignin, and other materials, chromosomes from certain organisms, DNA kinetoplasts in trypanosomes, chloroplasts, and many other structures.

We have used the terms *double refraction* and *birefringence* to refer to the ability of molecularly ordered objects to split an incident ray of light into two components, the O and E rays, but the two terms refer to different aspects of the same process. Double refraction refers to the visible phenomenon: the splitting of a single incident ray into two resultant rays as exemplified by a crystal of calcite. Birefringence refers to the cause of the splitting: the existence of direction-dependent variation in the refractive index in a molecularly ordered material. Birefringence B also refers to a measurable quantity, the difference in the refractive index $(n_e - n_o)$ experienced by the O and E rays during transit through an ordered object such that

$$B = (n_e - n_o).$$

Depending on the values of n_e and n_o, the *sign of birefringence* may be positive or negative, and specimens are therefore said to be either positively or negatively birefringent. Note also that birefringence is not a fixed value, but varies, depending on the orientation of the birefringent object relative to the illuminating beam of polarized light. We return to this important point in later sections.

Birefringence is related to another term, the *optical path difference* Δ (or in the field of polarized light, the *relative retardation* Γ), and both are defined as the relative phase shift expressed in nanometers between the O and E waves emergent from a birefringent object. As described in Chapters 5 and 7, the optical path length δ is given as $\delta = nt$, where n is the refractive index of a homogeneous medium between points A and B and t is the object thickness. Notice that the optical path length is a distance given in units of parameter t and that this term is equal to the geometric distance only when $n = 1$. The optical path difference Δ for two objects spanning the same distance is

$$\Delta = (n_1 - n_2)t.$$

Relative retardation and birefringence are related by the analogous expression

$$\Gamma = (n_e - n_o)t,$$

where t is the thickness, the physical distance traversed through the specimen. Accordingly, small and large objects may give the same retardation depending on the magnitude of their birefringence and physical size. Retardation can also be expressed as the mutual *phase shift* δ between the two wavelengths, and is given (in radians) by

$$\delta = 2\pi\Delta/\lambda.$$

Double refraction or birefringence is a property of polarizers used in a polarizing microscope and of microscope specimens that are active in polarized light. Its presence in a specimen allows us to measure the pattern and extent of molecular alignments, refractive index differences, and specimen thickness.

KINDS OF BIREFRINGENCE

Birefringence can be an inherent physical property of specimens such as the calcite crystal, or can be generated through cell biosynthetic activities (cellulose fibrils and starch granules in plant cells), or can arise from outside physical forces (cytoplasmic flow, cell movements) acting on components of an otherwise disorganized system. Various kinds of birefringence have been defined:

Intrinsic birefringence is based on the asymmetry of polarizability of chemical bonds within naturally occurring materials such as crystals. Examples: crystals of calcite and quartz.

Form birefringence or *structural birefringence* is associated with extensive ordered arrangements of macromolecular assemblies having dimensions and spacings comparable to the wavelength of light. Form birefringence is sensitive to the refractive index of the surrounding medium. Examples: parallel arrangements of actin and myosin filaments in muscle myofibrils, microtubule bundles in mitotic spindle fibers of dividing cells.

Flow birefringence refers to the induced alignment of asymmetric plate- or rod-shaped molecules in the presence of fluid flow or agitation. Examples: stirred solutions of detergents (shampoo), DNA, or flagella.

Strain birefringence describes the forced alignment of molecules in a transparent solid deformed by an externally applied force. Example: stretched films of polyvinyl alcohol.

Stress birefringence is descriptive when electronic deformation occurs in response to an external mechanical force without there being significant gross deformation. Example: a stressed lens caused by compression during mounting in a retaining ring or lens barrel.

PROPAGATION OF O AND E WAVEFRONTS IN A BIREFRINGENT CRYSTAL

In Chapter 3 we employed the concept of Huygens wavelets to describe the location of a secondary wavefront generated by spherical wavelets and originating from a point source of light in a homogeneous medium. In a transparent birefringent material, the ordinary or O ray behaves in the same way, generating a spherical wavefront. However, the extraordinary or E waves behave differently. As described by Huygens in 1690, the expanding wavefront of the E ray at a time t can be described as the surface of an ellipsoid (Fig. 8-8). An *ellipsoid* is the figure generated by rotating an ellipse about its major or minor axis. The ellipsoidal form indicates the presence of different velocities for the E ray along different trajectories in the crystal, where the upper- and lower-limit velocities define the long and short axes of the wavefront ellipsoid. The long axis corresponds to the direction along which the wavefront reaches its greatest possible velocity through the crystal, and is termed the *fast axis,* while the short axis corresponds to the direction giving the smallest velocity, and is called the *slow axis.* The velocities of waves traveling in all other directions have intermediate values. Since the velocity of light in a medium is described as $v = c/n,$ where c is the speed of light in a vacuum and n is the refractive index, we may infer that n is not constant in a birefringent crystal, but varies, depending on the path taken by a ray through the crystal. Several additional points about the propagation of wavefronts in a crystal are worth noting:

For uniaxial crystals, the O and E wavefronts coincide at either the slow or the fast axis of the ellipsoid, and the difference in surface wavefronts along the propagation axis is termed the optical path difference or relative retardation.

If the O and E wavefronts coincide at the major axis of the ellipsoid, $n_e > n_o$ in directions other than along the optic axis, and the specimen is said to be positively birefringent (Fig. 8-9). This is the case for crystals such as quartz and most ordered biological materials. For materials such as calcite, whose O and E wavefronts meet at the minor axis of the ellipsoid, $n_o > n_e$ in directions other than along the optic axis. Such materials are said to exhibit negative birefringence.

For the unique case that the incident illuminating beam is parallel or perpendicular to the optic axis of the crystal, the paths of O and E rays follow the same trajectory and exit the crystal at the same location. If the incident ray is parallel to the optic axis, the E ray behaves as an O ray; if the incident ray is perpendicular to the optic axis, the O and E ray components experience different optical paths.

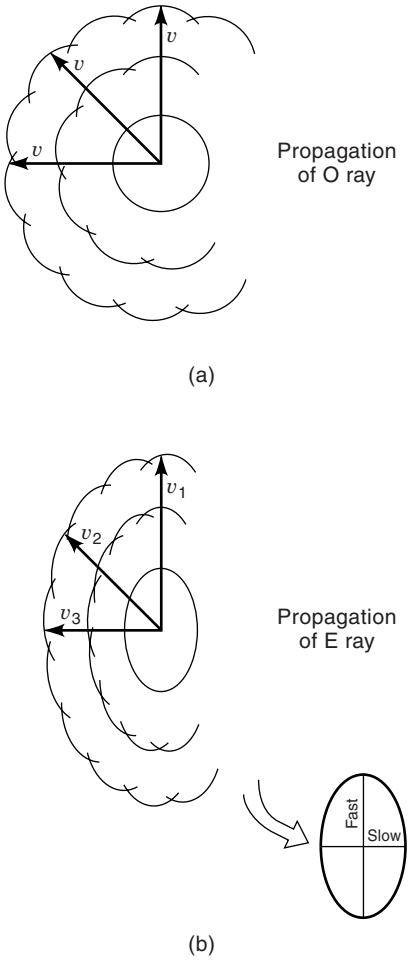

Figure 8-8

O and E rays emanating from a point in a birefringent material define spherical and ellipsoidal wavefronts. (a) The wavefront defined by O rays is spherical because the refractive index is uniform in all directions and waves propagate at a velocity given by the expression $v = c/n$. Circles are used to draw Huygens wavelets to depict the spherical wavefront. (b) The wavefront defined by the E rays is ellipsoidal because the refractive index n varies in different directions depending on the three-dimensional distribution of atoms and molecules. Since $v = c/n$, the velocity of the E rays is direction dependent (shown as v_1, v_2, v_3), resulting in a surface wavefront with the shape of an ellipsoid. Huygens wavelets are drawn using ellipses instead of circles to depict the advancing wavefront.

Double refraction is based on Maxwell s laws of electromagnetism. An explanation requires vector calculus and is beyond the scope of this text, but we can make a brief qualitative explanation of the principles involved. Since light contains both electric and magnetic components, the velocity of light in a medium depends in part on the electrical conductivity of the material and the interaction of light with electric fields in that medium, a property called the *dielectric constant* ϵ. For most dielectric substances and

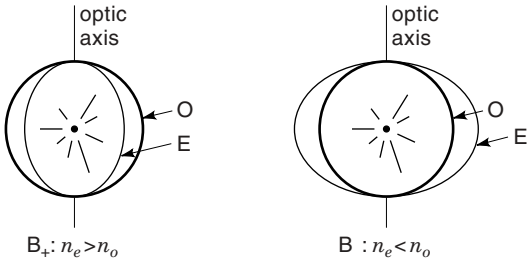

Figure 8-9
The relation of O and E wavefronts in specimens showing positive and negative birefringence.

biological materials, magnetic permeability is close to 1 and can be discounted; however, for materials with reduced magnetic permeability (metallic films), this would not be the case. The dielectric constant is related to the refractive index n by the simple relationship

$$\epsilon = n^2.$$

Therefore, in crystals having a particular lattice structure of atoms and molecules, the value of n is different in different directions, depending on the orientations of chemical bonds and electron clouds around atoms and molecules. The short axis (slow axis) of the wavefront ellipsoid corresponds to the axis defining the highest refractive index value; the long axis (fast axis) corresponds to the axis having the lowest refractive index value. The ellipsoid describing the orientation and relative magnitude of the refractive index in a crystal is called the *refractive index ellipsoid* or simply *index ellipsoid.*

BIREFRINGENCE IN BIOLOGICAL SPECIMENS

We have seen that the velocity of light during transit through a specimen is retarded by perturbations and interactions with electrons in the transmitting medium. The susceptibility of an electronic configuration to distortion is termed its *polarizability.* The more polarizable the electronic structure of a molecule, the more extensively light can interact with it, and, thus, the more slowly light is transmitted. In the extreme case, the interaction may be so strong that the specimen absorbs quanta of light.

Most chemical groups are asymmetric with respect to polarizability. For example, the electrons of carbon-carbon bonds in molecules with long carbon chains are most easily displaced along the direction of the bond (Fig. 8-10). A structure containing parallel chains of carbon-carbon bonds such as the cellulose polymers in cellophane is most polarizable in a direction parallel to the carbon chains. Since $\epsilon = n^2$, the velocity of light is lowest and the refractive index is highest in this direction. Therefore, when long carbon chain molecules are regularly oriented in biological structures as they are for example in cellulose fibers comprising a plant cell wall, the polarizability of the structure as a whole varies with its orientation in the illuminating beam of polarized light. As shown in Chapter 9, the orientation of the wavefront and index ellipsoids and the sign of birefringence of the specimen can be determined with the help of a compensator such as a full waveplate.

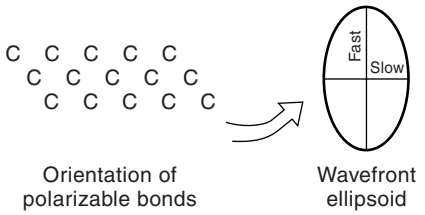

Figure 8-10

The axis of polarizability corresponds to the slow axis of the *wavefront ellipse.* In biological materials composed of linear arrays of macromolecules, the axis of strongest polarizability is usually determined by the direction of carbon-carbon bond alignments. Because polarizability and refractive index are highest in the direction parallel to the axis of bond alignment, this direction corresponds to the slow axis of the wavefront ellipsoid for this material.

GENERATION OF ELLIPTICALLY POLARIZED LIGHT BY BIREFRINGENT SPECIMENS

Birefringent objects split rays of incident light into separate O- and E-ray components whose E vectors vibrate in mutually perpendicular planes. The O and E waves comprising each ray or wave bundle also become mutually shifted in phase owing to differences in refractive index experienced by each wave during transit through the specimen. With the calcite crystal, we observed that the O and E rays follow different trajectories and emerge at widely separated locations on the surface of the crystal, making it relatively easy to examine each linearly polarized component separately with the aid of a Polaroid sheet. Let us now consider the circumstance where the optic axis of the specimen is perpendicular to the incident beam, which is the usual case for retardation plates and most biological specimens that are mounted on a microscope slide and examined in the object plane of the microscope. Because the incident ray is perpendicular to the optic axis of the specimen, the O and E rays follow the same trajectory as the incident ray, with one ray lagging behind the other and exhibiting a phase difference according to the amount of birefringence. Since the O and E waves vibrate in mutually perpendicular planes, they cannot interfere to produce a resultant wave with an altered amplitude. This point becomes important in polarization microscopy, because interference is required to generate a contrast image. As a convenience for describing the behavior of the superimposed wave pair, we may add the two waves together to form a single resultant ray. The mutually perpendicular orientation of the two E vectors and phase difference between the two rays result in a three-dimensional waveform called *elliptically polarized light.*

As seen in Figure 8-11, the E vector of the recombined wave does not vibrate in a plane over the course of its trajectory, but progressively rotates about its propagation axis. When viewed perpendicular to its propagation axis, the E vector appears to follow the course of an elliptical spiral, and when viewed end-on, the E vector sweeps out the shape of an ellipse. The resultant elliptical wave is reconstructed using simple vector addition in three-dimensional space. For O and E waves of equal amplitude, the amount of ellipticity depends on the amount of phase shift (Fig. 8-12). For phase shifts of exactly $\lambda/4$ and $3/4\lambda$, the shape of the resultant wave can be described as a circular spiral; for phase shifts of λ or $\lambda/2$, linearly polarized light results; for all other phase differences (the vast

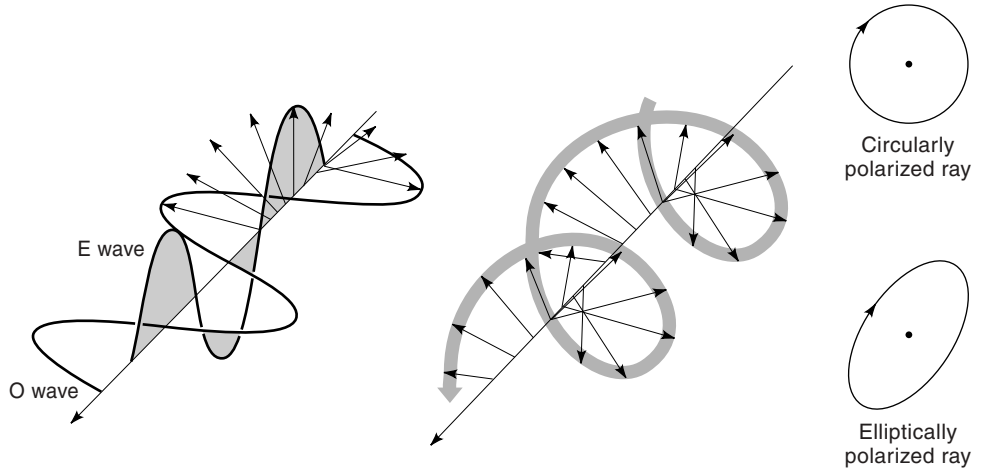

Figure 8-11

The waveforms of elliptically and circularly polarized light. O and E rays following the same propagation axis but vibrating in mutually perpendicular planes cannot interfere, but can be combined by vector addition. Depending on the relative phase difference between the two rays, the resultant wave may be linear or take on the form of a spiraling ellipse or circle. With a phase displacement of λ/4, the waveform is a circle.

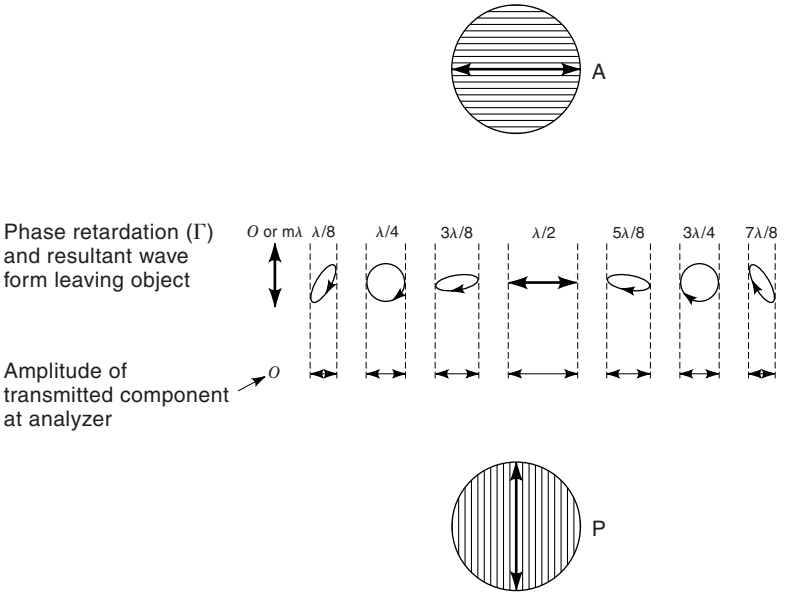

Figure 8-12

Effect of relative phase shift between O and E rays on the waveform of polarized light. Waves resulting from the combination of superimposed O and E rays have elliptical, spherical, or planar waveforms, depending on the amount of relative phase shift between the two rays. The orientations of the transmission axes of the polarizer and analyzer are indicated. The amplitudes of the components of vibration passing the analyzer are also shown.

majority), the shape is that of an elliptical spiral of varying degree of ellipticity. The component of elliptically polarized light that is able to pass through an analyzer varies depending on the amount of phase shift and is shown in Figure 8-12. The description of circular or elliptical waveforms is simply a convenient device for visualizing how O- and E-wave pairs interact with analyzers and optical elements called retardation plates.

Interference between two intersecting waves of light occurs only when their E vectors vibrate in the same plane at their point of intersection. Only when interference causes a change in the amplitude in the resultant wave can an object be perceived due to differences in intensity and contrast. The observed intensity from the O and E waves vibrating in mutually perpendicular planes emergent from a birefringent object is simply the sum of their individual intensities; no variations in intensity are observed because interference cannot occur and the object remains invisible. A sheet of cellophane held against a single polarizer on a light box is an example of this behavior. Cellophane is a birefringent sheet made up of parallel bundles of cellulose. The optic axis is parallel to the axis of the bundles and is contained in the plane of the sheet. When examined in polarized light without an analyzer, elliptically polarized light emerges from the cellophane, but since there is no interference or change in amplitude, the sheet remains invisible against the polarizer. However, if the cellophane is examined between two crossed polars, components of elliptical waves that are parallel to the analyzer are transmitted and emerge as linearly polarized light. Background rays from the polarizer are blocked by the analyzer, so the cellophane stands out as a bright object against a dark background. The sheet appears brightest when its optic axis is oriented at 45° with respect to the transmission axes of the two crossed polars.

CHAPTER

9

POLARIZATION MICROSCOPY

OVERVIEW

Image formation in the polarizing microscope is based on the unique ability of polarized light to interact with polarizable bonds of ordered molecules in a direction-sensitive manner. Perturbations to waves of polarized light from aligned molecules in an object result in phase retardations between sampling beams, which in turn allow interference-dependent changes in amplitude in the image plane. Thus, image formation is based not only on principles of diffraction and interference, but also on the existence of ordered molecular arrangements. The degree of order encountered in objects ranges from near-perfect crystals to loosely ordered associations of asymmetric molecules or molecular assemblies. In the polarizing microscope, such structures generally appear bright against a dark background (Fig. 9-1). Polarization microscopy has been used to study the form and dynamics of many ordered cellular structures, including:

Mitotic spindle fibers in dividing cells
Actin filament bundles in a variety of cell types
Actin and myosin filaments in the myofibrils of striated muscle cells
Condensed DNA in certain sperm nuclei
Kinetoplast DNA in the mitochondria of trypanosomes
Helical strands of cellulose fibers in plant cell walls
Condensates of starch and lignin in plant cells
Virus crystalloids and crystals of organic compounds in the cytoplasm of plant cells
Lipid bilayers of the cell plasma membrane and mitochondria

In many cases, polarization microscopy is the only available method for studying the structure, formation, and dynamics of labile macromolecular assemblies or examining the effects of chemicals, drugs, or environmental conditions on cellular structures in vivo. For additional examples of the application of polarized light in studies of mitosis, see Inoué and Oldenbourg (1998) and Oldenbourg (1996, 1999).